

CHAPTER 1

INTRODUCTION

1 INTRODUCTION

A gas turbine system extracts energy from a flow of hot gas produced by the combustion of gas or fuel oil in a stream of compressed air. The resulting gas will be directed over the turbine's blades, spinning the turbine, and mechanically powering the compressor. At the end of the process, the hot gas will be expanded back to the atmosphere through nozzle.

Flue gas is a waste exhausted to the outside air through the chimney stack from the combustion process in an industrial furnace, a power plant's steam-generating boiler, or other large combustion devices in power plant. Flue gas basically composed of carbon dioxide (CO₂) and water vapor as well as nitrogen and excess oxygen remaining from the intake combustion air. It also contains a small percentage of pollutants such as particulate matter, carbon monoxide, nitrogen oxides and sulfur oxides.

Based on the research done, flue gas is released to the environment at a high temperature usually up to 180°C for combined power plant and 580°C for gas turbine power plant. Thus, energy recovery is a significant process to convert the thermal energy into electricity.

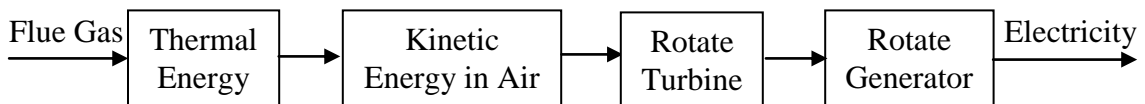


Figure 1.1: Energy Conversion of Thermal Energy into Electricity

1.1 Background of Study

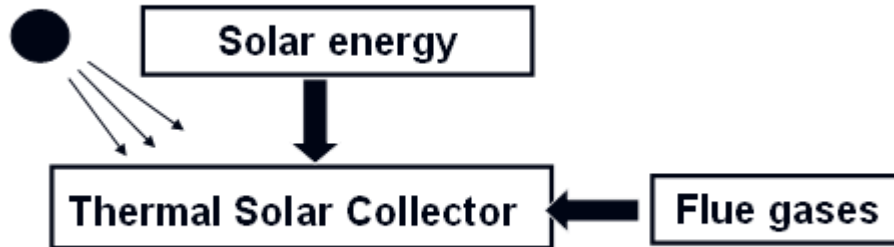


Figure 1.2: Energy Conversion of Thermal Energy into Electricity

This project aims to exploit the thermal energy of the flue gases discharged from the chimney stack at the power plant as an alternative source for solar energy due to the discontinues operation at night or during cloudy day. The thermal energy from the gases will be converted into kinetic energy to operate the Savonius wind rotor and then electricity by using a generator.

1.2 Problem Statement

The temperature of the flue gas discharged to the environment from combined power plant industry is ranging from 160 °C up to 180 °C. As for gas turbine power plant alone, the discharge temperature goes up to 700°C. As the global warming has become a major issue of the whole world now, it is important that this waste being exploited by conversion of the thermal energy to other useful type of energy to reduce the pollution and waste in the atmosphere. Another issue is due to the inaccessibility of solar thermal energy at night or during cloudy day. Thus, hot flue gas can be used as an alternative source of thermal energy.

1.3 Significance of Study

The global warming is one of the largest problems facing the future life in our planet, the Earth. Today, it has become the combination of technological and political issue. Increasing global temperature will cause sea level to rise and is expected to increase the intensity of extreme weather events and to change the amount of precipitation. All the human being is concern to contribute in reduction of this real fear facing the coming generation. Thus, a small reduction of temperature of the flue gas exit does contribute indirectly to reduce global warming in the world.

High discharged temperature of flue gas at the chimney stack is a valuable source of thermal energy and the biggest lost in the whole process. Therefore, the present work attempts to reduce the warming of atmosphere caused by flue gases exhausted from the thermal power plant. Besides that, the most important is to search for suitable simple technology for exploitation of this waste by converting to other useful type of energy such as electricity.

1.4 Objective

The objectives of this research are:

- To conduct analytical analysis of the energy recovery of flue gases to enhance solar chimney performance.
- To develop a lab scale model for experimental measurements of modified solar chimney backed up by thermal resource from waste flue gases of gas turbine.

1.5 Scope of the Work

In this research, there are two scope of studies required. First is to study the flue gas properties emitted from the stack chimneys as product of combustion in the power plant industry. Different properties of flue gas obtained from different type of burning substance. Thus for this research, the scope of study is focusing in combustion process in thermal power plant. In addition, study of the methods to control the temperature of flue gas necessitated to convert thermal energy into electricity is important.

Secondly, this research requires the study of heat transfer by convection to convert from thermal energy into kinetic energy to produce electricity. The panel used for this project acts as a heat exchanger. The electricity will be used to generate electricity 24 hours a day from the solar energy and thermal energy of flue gas.

CHAPTER 2

LITERATURE REVIEW

2 POWER PLANT INDUSTRY

A power plant station is an industrial area with facilities to generate electricity. It is known as the energy center because it describes what the plants do, which convert energy to other forms of energy, such as chemical energy, gravitational potential energy or heat energy into electrical energy.

Worldwide, most electric power is produced by steam-electric power plants that improve the overall efficiency producing about 86% of all electric generation [1]. The only other types of plants that currently have a significant contribution are hydroelectric and gas turbine plants, which can burn natural gas or diesel. Besides that, photovoltaic panels, wind turbines and binary cycle geothermal plants are also non-steam electric.

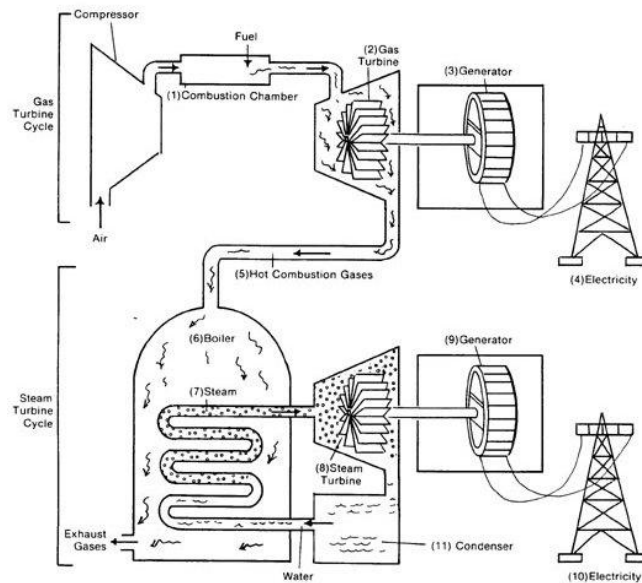


Figure 2.1: Combined Power Plant Cycle [2]

There are three types of power plant which produce flue gas from the combustion such as steam power plant, gas turbine power plant and combined power plant. Figure 2.1 shows the combined power plant where the upper part is the gas turbine cycle and the lower part is the steam power plant.

2.1 Fuels of Power Plant

In most of the power plant, fossil fuels are used to power the electric plants. Fossil fuels are made out of dead animals and plants that have been compressed in the earth for many years. Coal, petroleum and natural gas are three types of fossil fuels, which are not a renewable source of energy [3].

2.1.1 Coal

Coal is made from dead animals and leaves which takes millions of years to form. Coal is formed when the dead plants and animals have been put under a lot of pressure. The pressure of these overlying layers, as well as movements of the earth's crust and sometimes volcanic heat, acted to compress and harden the deposits to produce coal.

2.1.2 Petroleum

Petroleum is formed under the earth's surface by the decomposition of marine organisms. The remains of tiny organisms that live in the sea and plants that grow on the ocean bottoms are enmeshed with the fine sands and silts that settle to the bottom in quiet sea basins. The mud and sand harden into shale and sandstone; carbonate precipitates and skeletal shells harden into limestone; and the remains of the dead organisms are transformed into crude oil and natural gas.

2.1.3 Natural Gas

Natural gas contains valuable organic elements that are important raw materials of the natural-gasoline and chemical industries. Before natural gas is used as fuel, heavy hydrocarbons such as butane, propane, and natural gasoline are extracted as liquids. The remaining gas constitutes so-called dry gas, which is piped to domestic and industrial consumers for use as fuels; dry gas, devoid of butane and propane, also occurs in nature.

In this project, we are focusing on the Natural Gas which is the Liquefied Petroleum Gas (LPG). LPG is the mixture of gases, chiefly propane butane and propylene produced commercially from petroleum and stored under pressure to keep it in a liquid state. When prepared as fuel, LPG is largely propane contributing minimum 90% of LPG; common uses are for powering automotive vehicles, for cooking and heating, and sometimes for lighting in rural areas. At higher temperatures, propane burns in air, producing carbon dioxide and water as final products, and is valuable as a fuel. There are commercially three different grades of LPG. HD-5 Propane is widely used nowadays. The compositions of the LPG available are shown in Table 1.

Table 2.1: Composition of Liquefied Petroleum Gas Types [4]

Components	HD-5 Propane	Commercial Propane	Commercial B/P Mixture
Propane	90 % liquid volume (min)	Propane and / or propylene	Butanes and / or butylenes with
Propylene	5 % liquid volume (max)	-	propane and / or propylene
Butane and heavier HC	2.5 % liquid	2.5 liquid	-
Moisture content	Dryness test of NGPA	Dryness test of NGPA	-
Residual Matter	0.05 ml	0.05 ml	-
Pentane and heavier HC			2 % liquid volume (max)
Total sulfur	123 PPMW	185 PPMW	140 PPMW

*PPMW: Particles per million by weight fraction

2.2 Flue Gases of Power Plant

Flue gas is a gas discharged to the atmosphere at a high temperature via a passageway, which is a pipe or channel conveying exhaust gases from a fireplace, oven, furnace, boiler or steam generator at power plants. For this energy recovery research, it is important to determine the properties of flue gas discharged from the combustion. The most important properties acquired are the temperature, T (K) of the flue gas and its mass flow rate, \dot{m} (kg/s), which will be used to determine the rate of heat produced.

Flue gas produced in huge quantity has to be removed from the boiler furnaces through stack chimneys to the atmosphere. Based on research, in modern boilers, the fuel burning rate is high, and so the rate of air supply and the rate of flue gas removal are high as well. Appendix I shows the exhaust temperature of flue gases from different types of appliances.



Figure 2.2: Flue Gas Emission through Stack Chimney

There are a lot of waste heat sources such as Cement Plant, Petrochemical Plant, Refinery, Gas Power Plant, Coal Fired Power Plant, Furnace and many more as shown in Appendix II. All these plants and industries have contributed a lot to the increasing of global warming as well as pollution.

Studies show that the biggest contribution for waste heat comes from the Petrochemical Plant followed by Incineration Industry. It is believed that 19 % of the overall waste heat can be developed for power generation. The pie chart of the waste heat potential industry and waste heat recovery potential is shown in Figure 2.3.

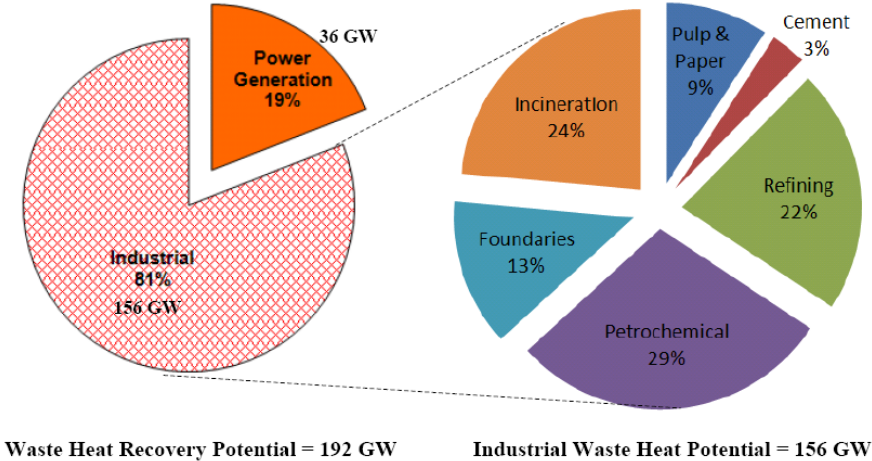


Figure 2.3: Electrical Power Generation Potential from Waste Heat Recovery [5]

According to Arvind Thekdi [6], “waste gas heat losses are an unavoidable part of operating any fuel-fired furnace, kiln, boiler, oven, or dryer. The flue gases still hold considerable thermal energy, often more than what was left behind in the process as the biggest loss in the whole process”. Therefore this statement clearly shows us that the exploitation for a recycled waste gas heat is essential. This research can be further developed as a renewable energy in the near future.

2.3 Energy Recovery by Recirculation of Flue Gases into the Furnace

A similar research work has been done for flue gas recirculation into the furnace or burner. Since flue gases still consists a considerable amount of heat, this technology uses 20% to 30% of the flue gases to be re-circulated and mixed with the combustion air. This will reduce the temperature and availability of oxygen to reduce thermal requirement.

This flue gas recirculation helps to improve the efficiency of the whole process such as the boiler's operating cycle. Besides that, this idea can improve the maintenance and combustion control. By re-circulating the flue gases, the system can minimize the heat losses as well as electrical energy of auxiliary systems. This is a new research boiler technology to improve the efficiency and at the same time reduce the heat losses.

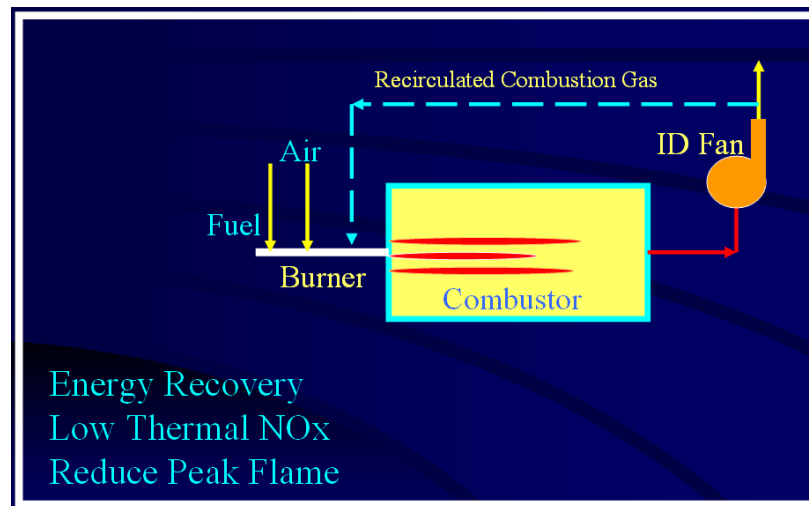


Figure 2.4: Energy Recovery by Circulation of Flue Gases into the Furnace [7]

2.4 Pipeline Compressor Station

This project mainly captures the heat from the wasted flue gases of several gas turbines at the pipeline compressor stations. The heat captured will be used to produce electricity. This project will be able to produce an output power of 9 MW. From the analysis, the heat recovery efficiencies will increase with Cascading Closed Loop Cycle (CCLC). The new technology is patented and called WOWGen with clean, zero emission system.

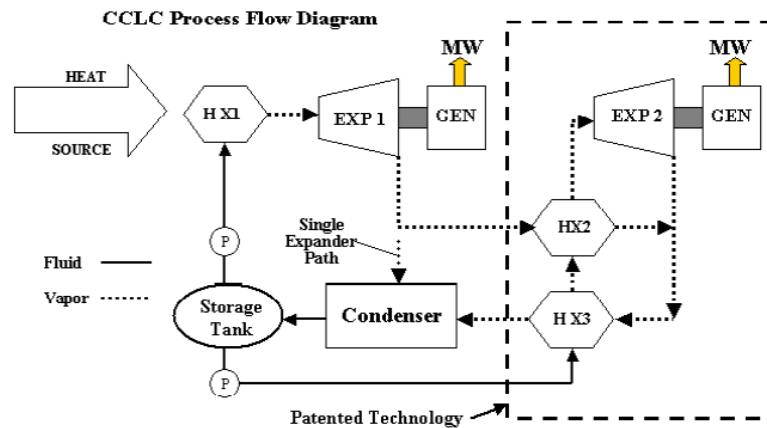


Figure 2.5: Energy Recovery for Other Application to Produce Electricity [5]

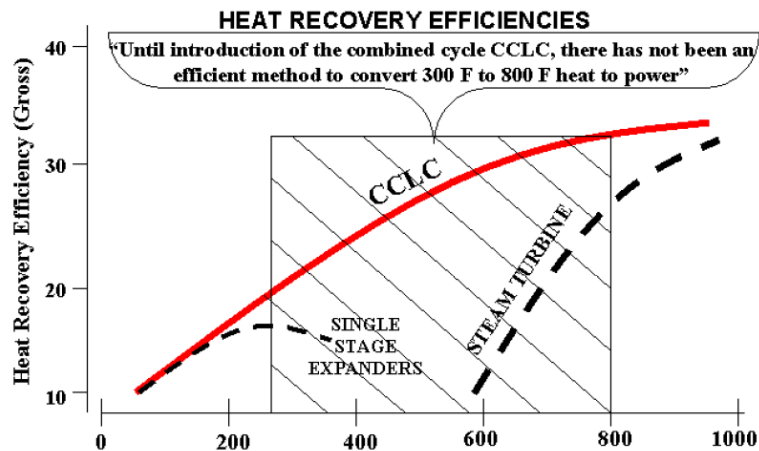


Figure 2.6: Heat Recovery Efficiencies by using CCLC [5]

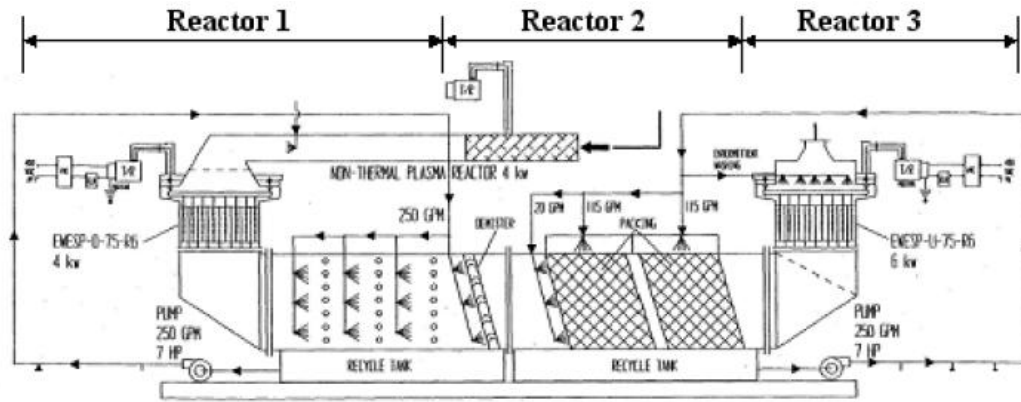


Figure 2.7: Heat Recovery System

From the figure, it is a combined dual cycle turbo-expander system. The system converts heat from the combustion of any fuel from a waste into electricity. This system converts renewable energy to power.

The main key features are:

- 95% NO_x and SO_x
- 85% mercury
- 90% vaporized heavy metals
- 99.5% particulate removal
- 25% CO₂

From the research, it is proven that wasted heat recovery is a significant future work since there is no technology which really exists to efficiently convert waste heat to power by using flue gases. Therefore the energy recovery of flue gases can be used as a source of thermal energy to improve the performance of a modified solar chimney.

CHAPTER 3

CONCEPTUAL DESIGN ANALYSIS

3 DESIGN SYSTEM

There are three main parts in the panel design system which are;

1. Panel Modeling
2. Savonius Wind Rotor
3. Chimney

The panel modeling acts as a heat exchanger to transfer the heat from hot flue gas to the air via convection. The hot air will increase the velocity in the air to rotate the Savonius wind rotor with a velocity at around 6 m/s. There will a chimney installed above the collector panel to create a buoyancy force. All the system design and parameters will be further discussed in the following to determine the best selection and configuration for the system

3.1 Heat Transfer

In thermal physics, heat transfer involves thermal energy from a hot to a colder body or vice versa. Whenever there is a temperature difference between two contacting body, transfer of thermal energy will occur or also known as heat exchange until a thermal equilibrium is achieved. Heat transfer usually occurs from a hot body to a cold one following second law of thermodynamics. For example, during the day time, heating of Earth's surface warms a very thin layer of air in contact with the surface. Above this thin laminar layer, air heated from below expands and rises upward because of the inherent buoyancy of warm air where heat transfer takes place.

3.2 Heat Transfer via Convection

Convection is a combination of conduction and the transfer of thermal energy by fluid circulation or movement from the hot particles in bulk to cooler areas in a material medium. Heat transfer via convection is accomplished by displacement or movement of the medium. As convection is dependant on the bulk movement of a fluid it can only occur in liquids, gases and multiphase mixtures.

Heat transfer by convection is split into two categories: natural convection and forced convection

3.2.1 Natural and Forced Convection

Natural convection is a type of heat transport in which the fluid motion is generated only by density differences in the fluid occurring due to temperature gradients. In natural convection, fluid surrounding a heat source receives heat, becomes less dense and rises. In free convection, fluid motion driving force is primarily due to buoyancy forces within the fluid. Buoyancy is caused by the combined pressure of a fluid density gradient and a body force that proportional to its density.

Mathematically, the tendency of a particular system towards natural convection relies on the Grashof number (Gr), which is a ratio of buoyancy force and viscous force.

$$Gr_L = \frac{g\beta (T_s - T_\infty) L^3}{\nu_{air}^2}$$

Transition in a free convection boundary layer depends on the relative magnitude of the buoyancy and viscous forces in the fluid. It is correlated to its occurrence in terms of Raleigh Number, Ra.

$$Ra = Gr.Pr \quad \text{where the transition point is at } Ra \sim 10^9$$

Forced convection is another type of heat transport in which fluid motion is generated by an external source such as a pump, fan and suction device. Forced convection is often encountered in designing or analyzing heat exchangers, pipe flow, and flow over a plate at a different temperature than the stream. However, in any forced convection situation, some amount of natural convection is always present. When the natural convection is not negligible, such flows are typically referred to as mixed convection.

When dealing with internal flow, it is important to be cognizant of the extent of the entry region, which depends on whether the flow is laminar or turbulent. The Reynolds number for flow in an enclosed tube is

$$Re = \frac{\rho.V.D_h}{\mu} \quad \text{where the transition point is at } Re \sim 2300$$

To determine if the flow is a natural or forced convection flow, we can calculate the Grashof and Reynolds number;

- $Gr_L/Re_L^2 \gg 1$ forced convection can be neglected
- $Gr_L/Re_L^2 = 1$ forced convection and natural convection must be considered
- $Gr_L/Re_L^2 \ll 1$ natural convection can be neglected

3.3 Heat Transfer by Forced Convection for Noncircular Enclosed Region

For circular tubes, D_h , is the diameter of the tubes. However, any of the applications nowadays, involve convection transport in noncircular tubes which will be using an effective diameter as the characteristic length. It is termed as hydraulic diameter and is defined as

$$D_h = 4A_c / P \quad (\text{non circular tubes})$$

where A_c is the flow cross-sectional area and P is the wetted perimeter. In this noncircular enclosed region, the coefficient is presumed to be an average over the perimeter.

For the convection heat transfer, Nusselt Number is a dimensionless parameter to the thermal boundary layer where the friction coefficient is the velocity boundary layer. From the knowledge of Nusselt Number, Nu , the local convection coefficient, h , may be found.

For laminar flow, the Nusselt Number can be obtained by using Appendix 1 [8]. As for turbulent flow, it is reasonable to use the circular tube correlation for fully develop flow. According to Dittus-Boelter equation, we can evaluate the Nusselt Number, Nu using the equations below

$$Nu_D = 0.0243 Re_D^{4/5} Pr^{0.4} \quad (\text{heating})$$

$$Nu_D = 0.0265 Re_D^{4/5} Pr^{0.3} \quad (\text{cooling})$$

After we determine the Nusselt Number, we can evaluate the convection coefficient, h .

$$h = \frac{Nu_D \cdot k}{D_h}$$

3.4 Energy Balance

Energy balance equation can be applied to determine how the mean temperature varies with position along an enclosed region. The total heat transfer via convection is then related to the difference in temperatures at the tube inlet and outlet. Therefore, the balance equation for convection heat transfer is given below

$$Q_{\text{conv}} = m \cdot c_p \cdot (T_{m,o} - T_{m,i})$$

Applying this equation to the differential control volume in Figure 3.1, mean temperature is defined such that $mc_p T_m$ represents the true rate of thermal energy or enthalpy advection integrated over the cross section.

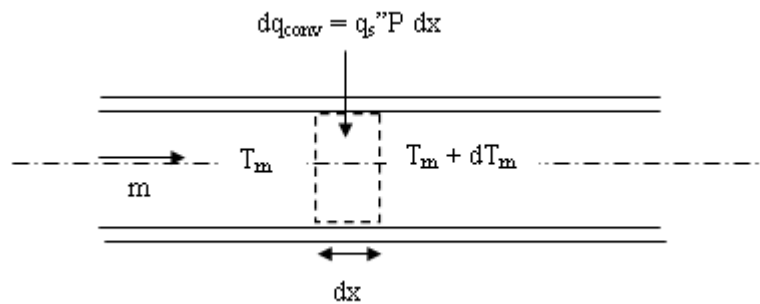


Figure 3.1: Control Volume for Internal Flow in a Conduit [8]

3.5 Corrugated Plate

A corrugated plate is arranged symmetrically with relation to its longitudinal axis, at an angle to it; at one end of the plate there are additional corrugations located, in the main, parallel to the longitudinal axis of the plate. This means that the crests and grooves of the corrugation are at least substantially horizontally oriented.



Figure 3.2: Corrugated Plate

Using a corrugate plate instead of flat plate as shown in Figure 3.2, we can increase the absorber plate area. This will increase the efficiency in heat absorbed.

$$\text{Corrugated Plate Area} \sim \pi/2 \times \text{Flat Area}$$

3.6 Savonius Wind Rotor

Savonius wind turbines are a type of vertical-axis wind turbine (VAWT), used to convert the power of the wind into torque on a rotating shaft. Savonius turbines are one of the simplest turbines. Aerodynamically, they are drag-type devices, consisting of two or three scoops. This rotor has an 'S' shape looking from the side in cross section. Due to its shape and configuration, the scoops experience less drag when moving against the wind than when moving with the wind. The Savonius rotor spin when there is differential drag and Savonius turbines extract much less of the wind's power than other similarly-sized lift-type turbines. Much of the swept area of a Savonius rotor is near the ground, making the overall energy extraction less effective due to lower wind speed at lower heights.

Savonius turbines are used whenever cost or reliability is much more important than efficiency. For example, most anemometers are Savonius turbines, because efficiency is completely irrelevant for that application. Much larger Savonius turbines have been used to generate electric power on deep-water buoys, which need small amounts of power and get very little maintenance. Design is simplified because, unlike horizontal-axis turbines, no pointing mechanism is required to allow for shifting wind direction and the turbine is self-starting.

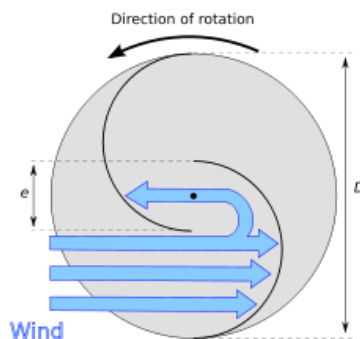


Figure 3.3: Savonius Rotor

Small Savonius wind turbines are sometimes seen used as advertising signs where the rotation helps to draw attention to the item advertised. They sometimes feature a simple two-frame animation.

3.7 Savonius Design

There are several variations of Savonius rotor design as shown below. The efficiency of a Savonius rotor is only around 15 % but they are ideal for many situations and can be increased depending on the configurations. Some variations are shown below, looking down from the top of the turbine.

3.7.1 Simple Configuration

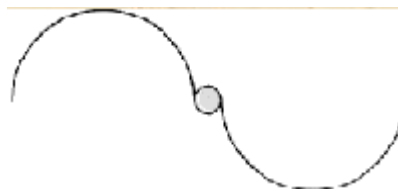


Figure 3.4: Simple Turbine Configuration

This configuration has a very strong due to the central shaft, but slightly less efficient than others. However, the extra strength allows the rotor to be supported at one end only.

3.7.2 Traditional Configuration



Figure 3.5: Traditional Turbine Configuration

This design is very simple and can be made easily from metal drums or pipe sections. The design is slightly more efficient than the simple configuration as some of the air is deflected by the second vane as it exits the first one.

3.7.3 Advanced Configuration



Figure 3.6: Advanced Turbine Configuration

This is the most efficient Savonius Design. It is not only having the advantage of air being deflected twice like the design above, but also that the vanes act partly like an airfoil when they are edge-on into the wind, creating a small lift effect and thus enhancing efficiency. This design is much more difficult to build requiring vanes rolled from metal sheet instead of being cut from drums or pipes.

Mathematical modeling has been developed for the Savonius rotor [9]. Two main factors affecting the performance of a Savonius rotor are Power Coefficient and Torque Coefficient as shown in the equation below

$$C_T = \frac{T}{0.5\rho R A_R V_W^2}$$

$$C_P = C_T \lambda$$

$$\lambda = \frac{V_R}{V_W}$$

$$\lambda = \frac{\omega \times R}{V_W}$$

where

C_T = Torque Coefficient

C_P = Power Coefficient

T = Torque

T = Torque produced by the rotor

ρ = Density of the air

R = Radius of the rotor ($D/2$)

V_W = Velocity of the wind approaching the rotor

λ = Tip Speed Ratio

ω = angular rotational speed of the rotor

3.8 Design Configuration

There are a few of improvements have been done to improve on the efficiency of the Savonius rotor especially on its installation.

3.8.1 Configuration 1

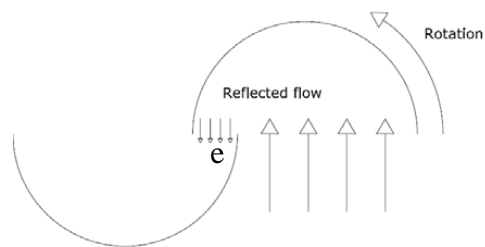


Figure 3.7: Configuration 1 - Two Rotor Cups Offset

The flow is deflected from concave down cup to concave down cup in the space by the offset of the two cups denoted in 'e', as shown in Figure 3.7.

3.8.2 Configuration 2

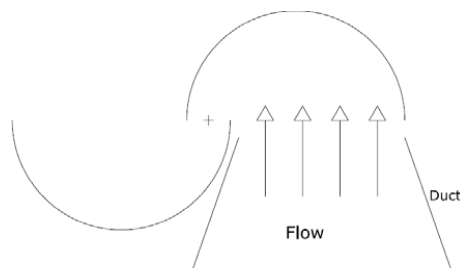


Figure 3.8: Configuration 2 - Flow Directed to the Concave Down Cup

The design of the air flowing to the concave up cup is has an upside down V shape to direct the flow to strike it, as shown in Figure 3.8.

3.8.3 Configuration 3

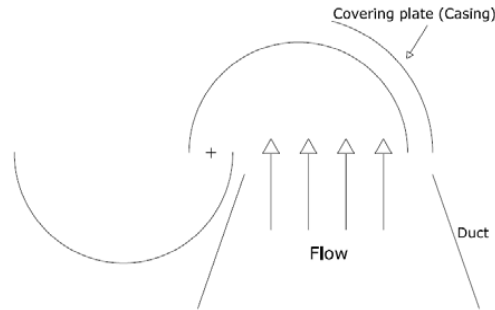


Figure 3.9: Configuration 3 – Curved Plate Installed Over the Concave Down Cup

For this configuration a curved plate is installed to cover the concave down cup. This plate act as a ‘Flow Controller’ causing the flow to be perpendicular to the projection area of the cup after 90° rotation as shown in Figure 3.9. This configuration will definitely produce a higher efficiency as compared to others.

The comparison of the results from researchers are summarized in Table 3.1

Table 3.1: Comparison of the Results of Savonius Installation Configuration [9]

Coefficients	Configuration 1	Configuration 2	Configuration 3
$C_{T,max}$	0.18	0.22	0.59
$C_{P,max}$	0.21	0.24	0.32

3.9 Chimney

A solar chimney is often referred to as a thermal chimney, is a way of improving the natural ventilation of buildings by using convection of air heated by passive solar energy. The thermal energy from the flue gas discharged from the power plant is taken up by the absorber plate. This will warm the air in its neighborhood which rises because of its buoyancy force drawing in ambient air to replace. As the warm air rises through the chimney, it gains velocity because of the constriction attaining its highest velocity in the throat of the nozzle.

According to Dr. Alan Williams [10], suitable dimensions and designs are very important such as the diameter of the throat to achieve highest velocity as well as the height of the chimney to increase the efficiency of the chimney.

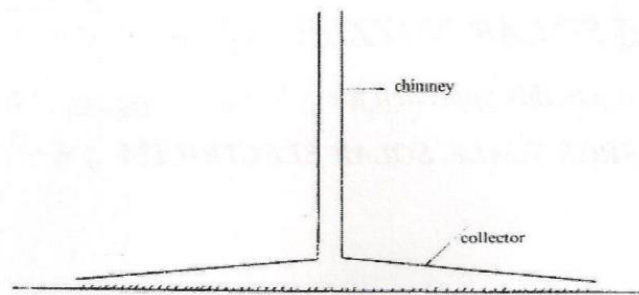


Figure 3.10: Chimney Design

The absorber plate is placed at the ground level under a large panel area. Warm air rises the gently sloping collector and then through the tall chimney. The main function of the chimney is to produce additional driving force which is the pressure difference. The overall pressure difference will create the buoyancy force driven by the air flow

$$\text{Buoyancy Force} = \rho g \Delta H$$

$$\text{Buoyancy Force} = \rho \cdot g \cdot (H_2 - H_1)$$

Improvement can be done to reduce the height of the chimney by reducing the outlet area. Padki and Sherif [11] suggested a small model chimney of radically different geometry as shown in Figure 3.11.

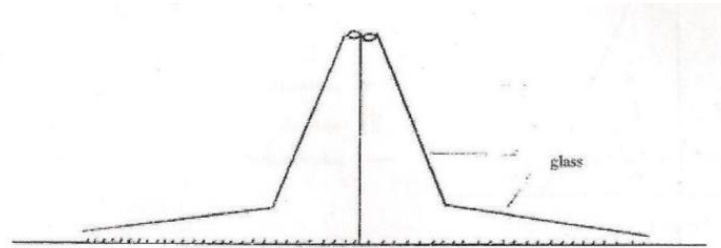


Figure 3.11: Improved Solar Chimney

In this case, the turbine is placed at the narrowing of the chimney. The velocity of air climbing the chimney is multiplied by A_1/A_2 where A_1 is the area base of the chimney and A_2 is the swept area of the turbine. The efficiency is multiplied by $(A_1/A_2)^2$. Based on theoretical research, the efficiency of the pressure drop is increased up to 20% as the A_1/A_2 ratio is increase.

CHAPTER 4

METHODOLOGY

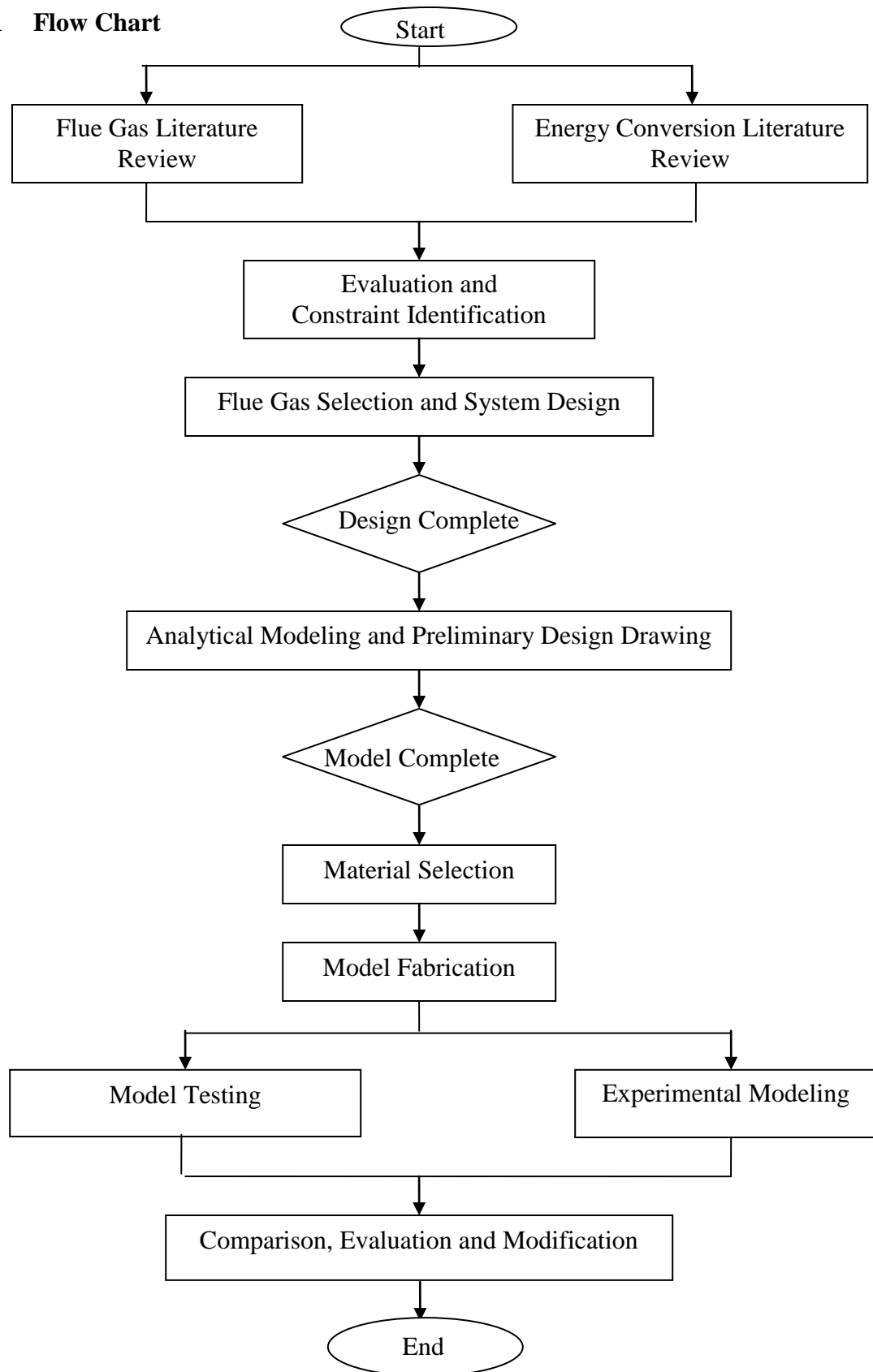
4 ANALYSIS TECHNIQUES

The methodology used to properly identify this energy recovery research consists of three steps;

1. Analytical
2. Model Fabrication
3. Experimental

Below are the Work Flow Chart throughout this energy recovery study and the Gantt Chart as the planned milestone for this project throughout the semester.

4.1 Flow Chart



Gantt Chart

CHAPTER 5

COMBUSTION ANALYSIS

5 INTRODUCTION

In large power plant, all the gas turbines and the steam generators as well as the process furnaces in large refineries, petrochemical and chemical plants and incinerators burn very considerable amounts of fossil fuels and therefore emit large amounts of flue gas to the ambient atmosphere. The total amounts of flue gas typically generated by the burning of fossil fuels such as natural gas, fuel oil and coal are shown in Table 2.2 which is obtained by stoichiometric calculations.

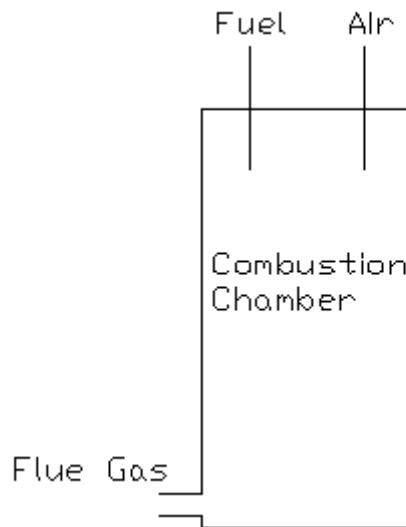
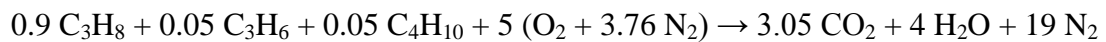


Figure 5.1: Fuel Combustion in the Chamber

For a complete combustion, the fuel will burn in oxygen in the air, producing a limited number of products as shown in Figure 5.1. When a hydrocarbon or any types of fuel burns in air, the combustion will yield carbon dioxide, nitrogen, water and some other common oxides.

Stoichiometric is the calculation of quantitative relationships of the reactants and products in chemical reactions. Stoichiometric is the minimum amount of air that supplies sufficient oxygen for the complete combustion of all the fuel. This indicates that no free oxygen would appear in the products of tailpipe emission. There are several stoichiometric combustion equations for different types of fuels used.

Stoichiometric combustion equation for LPG [4] [12];



The above theoretical chemical equation uses 5 moles of air with 1 mole of LPG for a complete combustion.

In this project, we take LPG as the combustion substance. From the stoichiometric equation, we can evaluate the properties of the flue gas at the exhaust. We can calculate the properties of an ideal gas mixture such as the specific heats, viscosity, thermal conductivity and others by using the conservation of energy principle in a system.

Since the internal energy and enthalpy of an ideal gas are functions of temperature only, the values of these properties for each component present in the mixture are determined by the mixture temperature alone. Accordingly,

$$U = U_1 + U_2 + U_3 + \dots + U_j$$

$$H = H_1 + H_2 + H_3 + \dots + H_j$$

where U_i and H_j are the internal energy and enthalpy of component i evaluated at the mixture temperature. In molar basis, the equation can be written as;

$$n\bar{u} = n_1\bar{u}_1 + n_2\bar{u}_2 + n_3\bar{u}_3 + \dots + n_j\bar{u}_j$$

$$n\bar{h} = n_1\bar{h}_1 + n_2\bar{h}_2 + n_3\bar{h}_3 + \dots + n_j\bar{h}_j$$

where \bar{u} and \bar{h} are the specific internal energy and specific enthalpy of the mixture per mole of mixture and n is the quantity of moles.

Thus, differentiating the equations above with respect to temperature results, we obtain the following expressions for the specific heats of the mixture on molar basis;

$$c_p = n_1c_{p1} + n_2c_{p2} + n_3c_{p3} + \dots + n_jc_{pj}$$

$$c_v = n_1c_{v1} + n_2c_{v2} + n_3c_{v3} + \dots + n_jc_{vj}$$

So, from the flue gas composition evaluated, we can calculate the properties of flue gas at exhaust based on the moles of each gas presents in the mixture.

Flue gas density, ρ and specific heat, c_p were evaluated using the following general equation taken from Moran and Shapiro [13].

$$\rho = \sum_{i=\alpha}^N y_\alpha \rho_\alpha$$

$$c_p = \sum_{i=\alpha}^N y_\alpha c_{p,\alpha}$$

where y is the mass fraction of the species.

The viscosity and thermal conductivity of the mixture is approximated by using [14];

$$\mu = \frac{\sum_{\alpha=1}^N x_{\alpha} \mu_{\alpha}}{\sum_{\beta} x_{\beta} \phi_{\alpha\beta}}$$

$$\phi_{\alpha\beta,\mu} = \frac{1}{\sqrt{8}} \left(1 + \frac{M_{\alpha}}{M_{\beta}} \right)^{\frac{-1}{2}} \left[1 + \left(\frac{\mu_{\alpha}}{\mu_{\beta}} \right)^{\frac{1}{2}} \left(\frac{M_{\beta}}{M_{\alpha}} \right)^{\frac{1}{4}} \right]^2$$

$$k = \frac{\sum_{\alpha=1}^N x_{\alpha} k_{\alpha}}{\sum_{\beta} x_{\beta} \phi_{\alpha\beta}}$$

$$\phi_{\alpha\beta,k} = \frac{1}{\sqrt{8}} \left(1 + \frac{M_{\alpha}}{M_{\beta}} \right)^{\frac{-1}{2}} \left[1 + \left(\frac{k_{\alpha}}{k_{\beta}} \right)^{\frac{1}{2}} \left(\frac{M_{\beta}}{M_{\alpha}} \right)^{\frac{1}{4}} \right]^2$$

where M is the species molar mass fraction, x is the mole fraction and α is the species number. For equation 2 and 3, p can be the viscosity or the thermal conductivity of the species.

The flue gas properties that are needed for the calculations are the density, specific heat, viscosity and heat transfer coefficient. From the properties, we can evaluate the Prandtl Number of the hot flue gas flow.

$$\text{Pr} = \frac{c_p \mu}{k}$$

where c_p is the specific heat, μ is the viscosity and k is the thermal conductivity.

5.1 Properties of Flue Gases

From the flue gas composition evaluated, we can calculate the properties of flue gas by using the thermo-physical properties of each substance in the gas at exhaust based on the moles of each gas presents in the mixture. The thermo-physical properties for CO₂, N₂ and H₂O are shown in Appendix III.

5.1.1 Steam Power Plant

For steam power plant, the exhaust temperature of the flue gases is approximately 450K (~ 180°C). The products of combustion are [4]:



At first, we need to key in all the necessary properties and data for each of the substances in the mixture such as the molar mass (kg/kmol) and number of moles (kmol). Compute the mass, percent of moles and percent of mass in the mixture for each substance as shown in the table below. This data can be used to calculate the density and specific heat of the flue gas. The Molar Mass, M and the number of moles are given in Table 5.1 for each species in the flue gas.

Table 5.1: Molar Mass and Number of Moles for CO₂, H₂O and N₂ in Flue Gas

Species	Molar Mass (kg/kmol)	No. Moles (kmol)
CO ₂	44.010	3.05
H ₂ O	18.015	4.00
N ₂	28.013	19.00
Total	90.038	26.05

Therefore, we can calculate the percentage of moles in the mixture using the following equation.

$$\begin{aligned}\text{For CO}_2, \quad \text{Mole \%} &= 3.05 / 26.05 \times 100 \% \\ \text{Mole \%} &= \underline{0.11708 \%}\end{aligned}$$

$$\begin{aligned}\text{For H}_2\text{O}, \quad \text{Mole \%} &= 4.00 / 26.05 \times 100 \% \\ \text{Mole \%} &= \underline{0.15355 \%}\end{aligned}$$

$$\begin{aligned}\text{For N}_2, \quad \text{Mole \%} &= 19.00 / 26.05 \times 100 \% \\ \text{Mole \%} &= \underline{0.72937 \%}\end{aligned}$$

The mass of each species is given is evaluated to calculate the total mass of the flue gas. The total mass of the flue gas is 414.984 kg.

Therefore, we can calculate the percentage of weight in the mixture using the following equation.

$$\begin{aligned}\text{For CO}_2, \quad \text{Mass \%} &= 15.716 / 414.984 \times 100 \% \\ \text{Mass \%} &= \underline{0.03787 \%}\end{aligned}$$

$$\begin{aligned}\text{For H}_2\text{O}, \quad \text{Mass \%} &= 11.065 / 414.984 \times 100 \% \\ \text{Mass \%} &= \underline{0.02666 \%}\end{aligned}$$

$$\begin{aligned}\text{For N}_2, \quad \text{Mass \%} &= 388.203 / 414.984 \times 100 \% \\ \text{Mass \%} &= \underline{0.93547 \%}\end{aligned}$$

The percentage of mixture by moles and by weight is given in Table 5.2.

Table 5.2: Percentage of Moles and Weight of Flue Gas

Species	Molar Mass (kg/kmol)	No. of Moles (kmol)	Molar Mass x % Moles (kg/kmol)	Mass (kg)	Mole % (mol %)	Mass % (wt %)
CO ₂	44.010	3.05	5.15280	15.716	0.11708	0.03787
H ₂ O	18.015	4.00	2.76622	11.065	0.15355	0.02666
N ₂	28.013	19.00	20.43175	388.203	0.72937	0.93547
Total	90.038	26.05	28.35077	414.984	1.00000	1.00000

We can evaluate the density and specific heat of the mixture using the equation

$$\rho = \sum_{i=\alpha}^N y_{\alpha} \rho_{\alpha}$$

For Density of Flue Gas,

$$\rho = 0.11708 (1.1782 \text{ kg/m}^3) + 0.15355 (0.4902 \text{ kg/m}^3) + 0.72937 (0.7485 \text{ kg/m}^3)$$

$$\rho = \underline{\underline{0.7579 \text{ kg/m}^3}}$$

$$c_p = \sum_{i=\alpha}^N y_{\alpha} c_{p,\alpha}$$

For Specific Heat of Flue Gas,

$$c_p = 0.11708 (981 \text{ J/kg.K}) + 0.15355 (1980 \text{ J/kg.K}) + 0.72937 (1050 \text{ J/kg.K})$$

$$c_p = \underline{\underline{1072.1838 \text{ J/kg.K}}}$$

To evaluate viscosity and thermal conductivity of the flue gas, we must use a different equation following the transport phenomena equation.

For Viscosity of Flue Gas,

Let $\alpha = \text{CO}_2$,

$\beta = \text{CO}_2, \text{H}_2\text{O}$ and N_2

$$M_\alpha / M_\beta = 44.010 / 44.010 = 1.0000$$

$$M_\alpha / M_\beta = 44.010 / 18.015 = 2.4430$$

$$M_\alpha / M_\beta = 44.010 / 28.013 = 1.5711$$

$$\mu_\alpha / \mu_\beta = 0.0000210 / 0.0000210 = 1.0000$$

$$\mu_\alpha / \mu_\beta = 0.0000210 / 0.00001525 = 1.3770$$

$$\mu_\alpha / \mu_\beta = 0.0000210 / 0.00002396 = 0.8765$$

$$\phi_{\alpha\beta,\mu} = \frac{1}{\sqrt{8}}(1 + 1.0000)^{\frac{-1}{2}} \left[1 + (1.0000)^{\frac{1}{2}} (1.0000)^{\frac{1}{4}} \right]^2$$

$$\phi_{\alpha\beta,\mu} = \underline{1.0000}$$

$$\phi_{\alpha\beta,\mu} = \frac{1}{\sqrt{8}}(1 + 2.4430)^{\frac{-1}{2}} \left[1 + (1.3770)^{\frac{1}{2}} (2.4430)^{\frac{1}{4}} \right]^2$$

$$\phi_{\alpha\beta,\mu} = \underline{0.7161}$$

$$\phi_{\alpha\beta,\mu} = \frac{1}{\sqrt{8}}(1 + 1.5711)^{\frac{-1}{2}} \left[1 + (0.8765)^{\frac{1}{2}} (1.5711)^{\frac{1}{4}} \right]^2$$

$$\phi_{\alpha\beta,\mu} = \underline{0.7434}$$

$$\sum x_\beta \phi_{\alpha\beta} = 0.11708 \times 1.0000 + 0.15355 \times 0.7161 + 0.72937 \times 0.7434$$

$$\sum x_\beta \phi_{\alpha\beta} = \underline{0.7693}$$

Let $\alpha = \text{H}_2\text{O}$,
 $\beta = \text{CO}_2, \text{H}_2\text{O}$ and N_2

$$M_\alpha / M_\beta = 18.015 / 44.010 = 0.4093$$

$$M_\alpha / M_\beta = 18.015 / 18.015 = 1.0000$$

$$M_\alpha / M_\beta = 18.015 / 28.013 = 0.6431$$

$$\mu_\alpha / \mu_\beta = 0.00001525 / 0.0000210 = 0.7262$$

$$\mu_\alpha / \mu_\beta = 0.00001525 / 0.00001525 = 1.0000$$

$$\mu_\alpha / \mu_\beta = 0.00001525 / 0.00002396 = 0.6365$$

$$\phi_{\alpha\beta,\mu} = \frac{1}{\sqrt{8}} (1 + 0.4093)^{\frac{-1}{2}} \left[1 + (0.7262)^{\frac{1}{2}} (0.4093)^{\frac{1}{4}} \right]^2$$

$$\phi_{\alpha\beta,\mu} = \underline{1.2704}$$

$$\phi_{\alpha\beta,\mu} = \frac{1}{\sqrt{8}} (1 + 1.0000)^{\frac{-1}{2}} \left[1 + (1.0000)^{\frac{1}{2}} (1.0000)^{\frac{1}{4}} \right]^2$$

$$\phi_{\alpha\beta,\mu} = \underline{1.0000}$$

$$\phi_{\alpha\beta,\mu} = \frac{1}{\sqrt{8}} (1 + 0.6431)^{\frac{-1}{2}} \left[1 + (0.6365)^{\frac{1}{2}} (0.6431)^{\frac{1}{4}} \right]^2$$

$$\phi_{\alpha\beta,\mu} = \underline{0.9862}$$

$$\sum x_\beta \phi_{\alpha\beta} = 0.11708 \times 1.2704 + 0.15355 \times 1.0000 + 0.72937 \times 0.9862$$

$$\sum x_\beta \phi_{\alpha\beta} = \underline{1.0216}$$

Let $\alpha = \text{N}_2$,
 $\beta = \text{CO}_2, \text{H}_2\text{O}$ and N_2

$$M_\alpha / M_\beta = 28.013 / 44.010 = 0.6365$$

$$M_\alpha / M_\beta = 28.013 / 18.015 = 1.5550$$

$$M_\alpha / M_\beta = 28.013 / 28.013 = 1.0000$$

$$\mu_\alpha / \mu_\beta = 0.00002396 / 0.0000210 = 1.1410$$

$$\mu_\alpha / \mu_\beta = 0.00002396 / 0.00001525 = 1.5711$$

$$\mu_\alpha / \mu_\beta = 0.00002396 / 0.00002396 = 1.0000$$

$$\phi_{\alpha\beta,\mu} = \frac{1}{\sqrt{8}} (1 + 0.6365)^{\frac{-1}{2}} \left[1 + (1.1410)^{\frac{1}{2}} (0.6365)^{\frac{1}{4}} \right]^2$$

$$\phi_{\alpha\beta,\mu} = \underline{1.3326}$$

$$\phi_{\alpha\beta,\mu} = \frac{1}{\sqrt{8}} (1 + 1.5550)^{\frac{-1}{2}} \left[1 + (1.5711)^{\frac{1}{2}} (1.5550)^{\frac{1}{4}} \right]^2$$

$$\phi_{\alpha\beta,\mu} = \underline{0.9964}$$

$$\phi_{\alpha\beta,\mu} = \frac{1}{\sqrt{8}} (1 + 1.0000)^{\frac{-1}{2}} \left[1 + (1.0000)^{\frac{1}{2}} (1.0000)^{\frac{1}{4}} \right]^2$$

$$\phi_{\alpha\beta,\mu} = \underline{1.0000}$$

$$\sum x_\beta \phi_{\alpha\beta} = 0.11708 \times 1.3326 + 0.15355 \times 0.9964 + 0.72937 \times 1.0000$$

$$\sum x_\beta \phi_{\alpha\beta} = \underline{1.0384}$$

$$\mu = \sum_{\alpha=1}^N \frac{0.11708 \times 0.0000210}{0.7693} + \frac{0.15355 \times 0.00001525}{1.0216} + \frac{0.72937 \times 0.00002396}{1.0384}$$

$$\mu = \underline{\mathbf{0.00002232 \text{ kg/m.s}}}$$

For Thermal Conductivity of Flue Gas,

Let $\alpha = \text{CO}_2$,

$\beta = \text{CO}_2, \text{H}_2\text{O}$ and N_2

$$M_\alpha / M_\beta = 44.010 / 44.010 = 1.0000$$

$$M_\alpha / M_\beta = 44.010 / 18.015 = 2.4430$$

$$M_\alpha / M_\beta = 44.010 / 28.013 = 1.5711$$

$$k_\alpha / k_\beta = 0.0283 / 0.0283 = 1.0000$$

$$k_\alpha / k_\beta = 0.0283 / 0.0299 = 0.9465$$

$$k_\alpha / k_\beta = 0.0283 / 0.0358 = 0.7905$$

$$\phi_{\alpha\beta,\mu} = \frac{1}{\sqrt{8}}(1 + 1.0000)^{\frac{-1}{2}} \left[1 + (1.0000)^{\frac{1}{2}} (1.0000)^{\frac{1}{4}} \right]^2$$

$$\phi_{\alpha\beta,\mu} = \underline{1.0000}$$

$$\phi_{\alpha\beta,\mu} = \frac{1}{\sqrt{8}}(1 + 2.4430)^{\frac{-1}{2}} \left[1 + (0.9465)^{\frac{1}{2}} (2.4430)^{\frac{1}{4}} \right]^2$$

$$\phi_{\alpha\beta,\mu} = \underline{0.6025}$$

$$\phi_{\alpha\beta,\mu} = \frac{1}{\sqrt{8}}(1 + 1.5711)^{\frac{-1}{2}} \left[1 + (0.7905)^{\frac{1}{2}} (1.5711)^{\frac{1}{4}} \right]^2$$

$$\phi_{\alpha\beta,\mu} = \underline{0.7098}$$

$$\sum x_\beta \phi_{\alpha\beta} = 0.11708 \times 1.0000 + 0.15355 \times 0.6025 + 0.72937 \times 0.7098$$

$$\sum x_\beta \phi_{\alpha\beta} = \underline{0.7273}$$

Let $\alpha = \text{H}_2\text{O}$,
 $\beta = \text{CO}_2, \text{H}_2\text{O}$ and N_2

$$M_\alpha / M_\beta = 18.015 / 44.010 = 0.4093$$

$$M_\alpha / M_\beta = 18.015 / 18.015 = 1.0000$$

$$M_\alpha / M_\beta = 18.015 / 28.013 = 0.6431$$

$$k_\alpha / k_\beta = 0.0299 / 0.0283 = 1.0565$$

$$k_\alpha / k_\beta = 0.0299 / 0.0299 = 1.0000$$

$$k_\alpha / k_\beta = 0.0299 / 0.0358 = 0.8352$$

$$\phi_{\alpha\beta,\mu} = \frac{1}{\sqrt{8}}(1 + 0.4093)^{\frac{-1}{2}} \left[1 + (1.0565)^{\frac{1}{2}} (0.4093)^{\frac{1}{4}} \right]^2$$

$$\phi_{\alpha\beta,\mu} = \underline{1.5550}$$

$$\phi_{\alpha\beta,\mu} = \frac{1}{\sqrt{8}}(1 + 1.0000)^{\frac{-1}{2}} \left[1 + (1.0000)^{\frac{1}{2}} (1.0000)^{\frac{1}{4}} \right]^2$$

$$\phi_{\alpha\beta,\mu} = \underline{1.0000}$$

$$\phi_{\alpha\beta,\mu} = \frac{1}{\sqrt{8}}(1 + 0.6431)^{\frac{-1}{2}} \left[1 + (0.8352)^{\frac{1}{2}} (0.6431)^{\frac{1}{4}} \right]^2$$

$$\phi_{\alpha\beta,\mu} = \underline{1.1260}$$

$$\sum x_\beta \phi_{\alpha\beta} = 0.11708 \times 1.5550 + 0.15355 \times 1.0000 + 0.72937 \times 1.1260$$

$$\sum x_\beta \phi_{\alpha\beta} = \underline{1.1569}$$

Let $\alpha = \text{N}_2$,
 $\beta = \text{CO}_2, \text{H}_2\text{O}$ and N_2

$$M_\alpha / M_\beta = 28.013 / 44.010 = 0.6365$$

$$M_\alpha / M_\beta = 28.013 / 18.015 = 1.5550$$

$$M_\alpha / M_\beta = 28.013 / 28.013 = 1.0000$$

$$k_\alpha / k_\beta = 0.0358 / 0.0283 = 1.2650$$

$$k_\alpha / k_\beta = 0.0358 / 0.0299 = 1.1973$$

$$k_\alpha / k_\beta = 0.0358 / 0.0358 = 1.0000$$

$$\phi_{\alpha\beta,\mu} = \frac{1}{\sqrt{8}} (1 + 0.6365)^{\frac{-1}{2}} \left[1 + (1.2650)^{\frac{1}{2}} (0.6365)^{\frac{1}{4}} \right]^2$$

$$\phi_{\alpha\beta,\mu} = \underline{1.4106}$$

$$\phi_{\alpha\beta,\mu} = \frac{1}{\sqrt{8}} (1 + 1.5550)^{\frac{-1}{2}} \left[1 + (1.1973)^{\frac{1}{2}} (1.5550)^{\frac{1}{4}} \right]^2$$

$$\phi_{\alpha\beta,\mu} = \underline{0.8670}$$

$$\phi_{\alpha\beta,\mu} = \frac{1}{\sqrt{8}} (1 + 1.0000)^{\frac{-1}{2}} \left[1 + (1.0000)^{\frac{1}{2}} (1.0000)^{\frac{1}{4}} \right]^2$$

$$\phi_{\alpha\beta,\mu} = \underline{1.0000}$$

$$\sum x_\beta \phi_{\alpha\beta} = 0.11708 \times 1.4106 + 0.15355 \times 0.8670 + 0.72937 \times 1.0000$$

$$\sum x_\beta \phi_{\alpha\beta} = \underline{1.0277}$$

$$k = \sum_{\alpha=1}^N \frac{0.11708 \times 0.0283}{0.7273} + \frac{0.15355 \times 0.0299}{1.1569} + \frac{0.72937 \times 0.0358}{1.0277}$$

$$k = \underline{\mathbf{0.0339 \text{ W/m.K}}}$$

For Prandtl Number of Flue Gas,

$$\text{Pr} = \frac{c_p \mu}{k}$$

$$\text{Pr} = \frac{1072.1838 \times 0.00002232}{0.0339}$$

$$\text{Pr} = \underline{\underline{\mathbf{0.7052}}}$$

The same equation is being used to determine the properties of the flue gas at higher temperature around 850K for gas turbine power plant. The results are tabulated in Table 5.3 to be used for the thermo fluid analysis in the energy conversion processes.

Table 5.3: Thermo physical Properties of Flue Gas

Properties	Steam Power Plant at T = 450 K	Gas Turbine Power Plant at T = 850 K
Density, ρ (kg/m ³)	0.7579	0.4263
Specific Heat, c_p (J/kg.K)	1072.1838	1242.9567
Viscosity, μ (kg/m.s)	0.00002232	0.00003384
Thermal Conductivity, k (W/m.K)	0.0339	0.0556
Prandtl Number, Pr	0.7052	0.7562

CHAPTER 6

DETAIL DESIGN ANALYSIS

6 DESIGN CONCEPT AND FABRICATION

The design of this project implements the concept of a solar panel. There will be two passageways; one for the flue gas and the other one for the air. The main collector also acts as a heat exchanger.

6.1 Geometry of the Rig

After the combustion analysis and the thermo fluid analysis, below shows the parameters for the proposed design.

Table 6.1: Dimensions for the Panel

Flue Gas Passage	Width (m)	1.00
	Length (m)	1.50
	Height (m)	0.05
Air Passage	Width (m)	1.00
	Length (m)	1.50
	Height (m)	0.05
Absorber	Width (m)	1.00
	Length (m)	1.50
	Thickness (m)	0.009
Savonius Rotor	Diameter (m)	0.04
	Length (m)	1.00
Chimney	Height (m)	1.00
	Base length (m)	1.00
	Top length (m)	0.20
	Width (m)	0.30

6.2 Design Criteria of the Main Component

There are three main parts for this project which are the collector, Savonius rotor and chimney. The diagrams for all the main components are shown as below with detailed explanations. The real pictures set up in the laboratory for experimental work are shown in Appendix IV.

6.2.1 The Main Body (Collector Part)

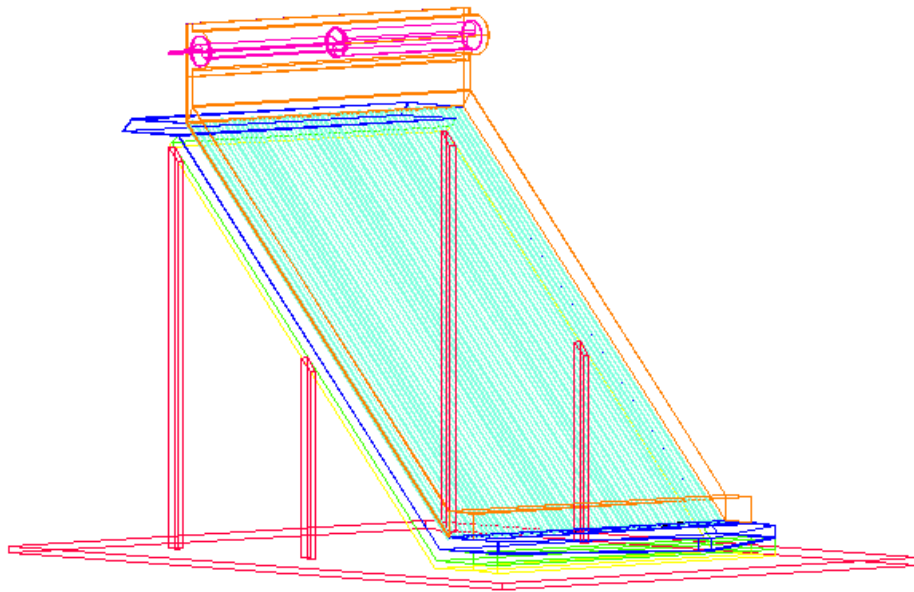


Figure 6.1: Proposed Panel Design

The main collector consists of two passageways; one for the flue gas and another one for the air. For the flue gas passageway, there is a triangular shape opening to guide the flue gas when flowing into the panel. This design is proposed in such a way so that the mass flow rate of the flue gas can be controlled. The mass flow rate of the flue gas will become constant at the beginning of the panel.

As for the entrance of the air passageway, it has a wider opening area to allow more air entering the panel.

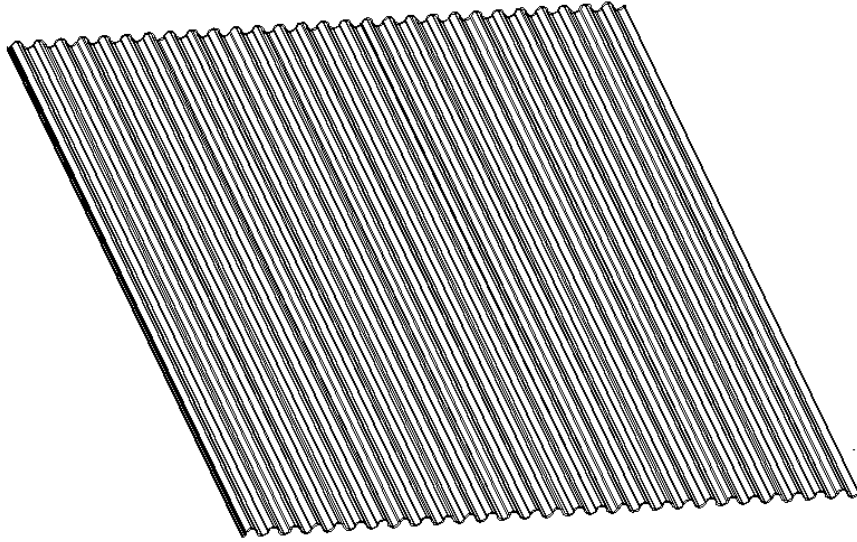


Figure 6.2: Corrugated Shape Absorber

In this project, it is proposed to use a corrugated plate absorber to increase the absorbing area.

6.2.2 The Turbine Section

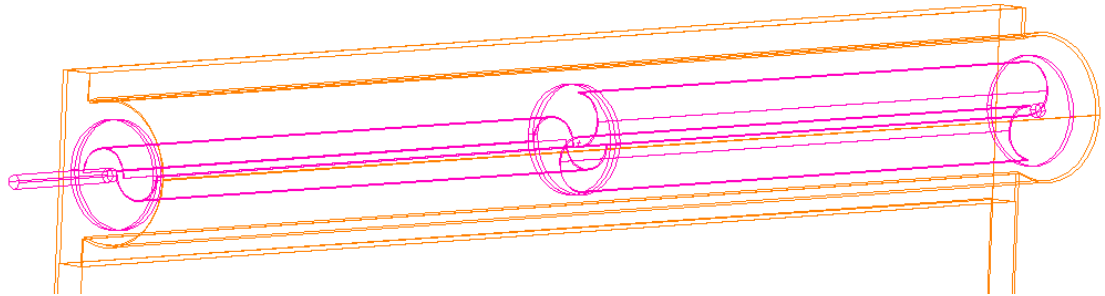


Figure 6.3: Proposed Savonius Wind Rotor Design

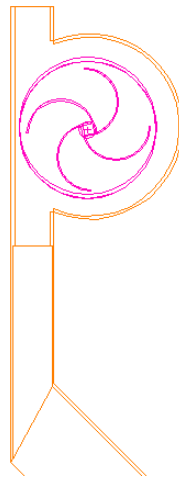


Figure 6.4: Side View of the Savonius Wind rotor

The Savonius wind rotor is fabricated into two parts that are perpendicular with each other to achieve eccentricity.

6.2.3 The Chimney Section

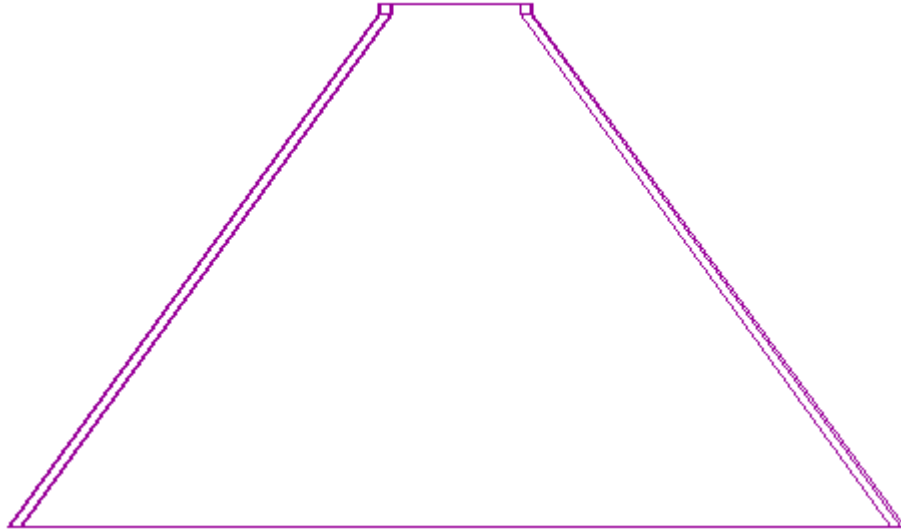


Figure 6.5: Proposed Chimney Design

For the design of the chimney section, it is proposed to have a conical shape chimney with a narrowing end. This chimney acts as a nozzle. According to Bernoulli's Law, by reducing the area at the end part of the chimney, the velocity will increase. The increase in velocity will reduce the pressure at the outlet of the chimney and thus increasing the pressure drop in the chimney. The main reason for having this design is to reduce the height of the chimney. This configuration requires a taller square shape chimney in order to produce the same pressure drop.

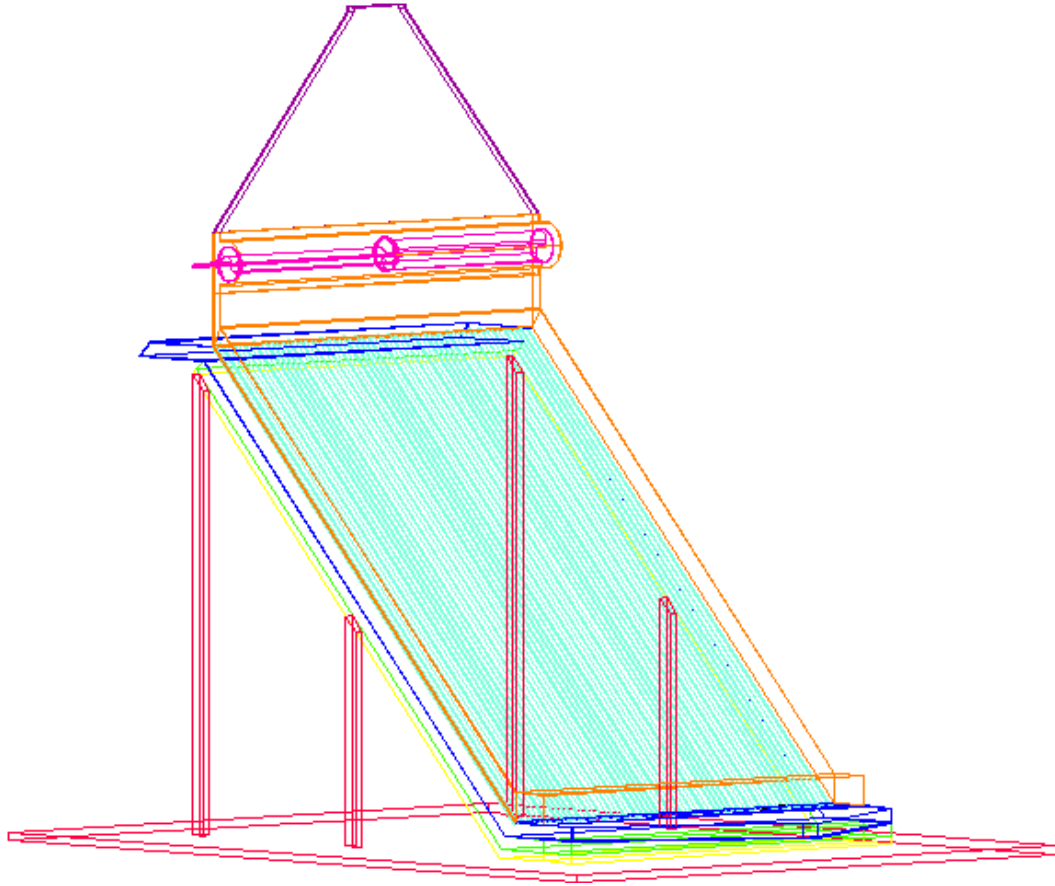


Figure 6.6: Proposed Panel Design

The hot flue gases discharged from the power plant will pass through the underneath passageway. The heat will be absorbed by the absorber plate and transfer to the air flowing in the passage above the absorber. The absorber is made up of corrugated shape to enhance the heat absorbing efficiency. The air will be heated up and directed to the top of the panel converting from thermal energy into kinetic energy. This kinetic energy will be able to rotate the Savonius rotor to generate electricity. There will be a chimney installed at the top part of the panel to create upward buoyancy force for additional power to rotate the Savonius wind rotor.

6.3 Material Selection for Main Components

Before the fabrication process, we need to determine the suitable material for each component.

6.3.1 Ply Wood

The first layer of the design is made of ply wood. Ply wood is made from thin sheets of wood that are attached to each other to improve its strength. In the design, ply wood is being used to provide good support to the panel and to act as a base for the insulator.

Advantages of Ply Wood:

1. It has a high uniform strength with the crossing of adjacent layers to equalize the strength.
2. It has a non-splitting quality as a supporter.
3. It is widely available in large sizes.
4. It is economical and relatively cheap
5. It makes the fabrication process much easier into the desired shapes.

Ply Wood is chosen because this application needs high quality material to avoid cracking, warping, shrinkage, breaking and twisting.

6.3.2 Asbestos Insulator

Asbestos that is a non-combustible material made up of minerals with long thin flexible fibrous crystal. The reasons for choosing asbestos as the insulator are:

- Sound absorption
- High tensile strength
- Low conductivity
- Withstand high temperature up to 1400°C
- Resistance to heat, chemical and electrical

6.3.3 Flue gas panel

The inlet and outlet of the flue gas passage, the material used is Galvanized Iron (GI) plate. GI plate is capable to withstand elevated temperature and with a high melting point.

6.3.4 Aluminum Absorber

In this design, absorber is placed between the flue gas passage and the air. Absorber is used to absorb the heat; a form of energy from the flue gas to be transferred to the air. The absorber for this design is proposed to have a corrugated shape to increase the absorbing surface area. Selective coating is applied to improve the efficiency of the absorber.

Only aluminum and zinc having corrugated shape of plate that are widely available in the market although copper would be more preferable. Therefore comparing between aluminum and zinc, aluminum plate is chosen due to its high melting temperature.

Reasons for choosing Aluminum Plate:

- Widely available in corrugated shape
- Cheaper than copper
- High melting point
- Less corrosion

Table 6.2: Physical Properties for Aluminum

Physical Properties	
Phase	Solid
Melting Point	933.47 K (660.32 °C, 1220.58 °F)
Boiling point	2792 K (2519 °C, 4566 °F)
Specific heat capacity (25 °C)	24.200 J/mol.K
Density	2.70 g/cm ³

To increase the absorbing efficiency, the panel can use copper absorber painted in black. However, a corrugated copper plate will have to be customized.

6.3.5 Perspex

Perspex is first introduced in 1930. Perspex is a clear, less weighted, thick and hard plastic. It is available in several thicknesses. It is transparent and has higher strength than normal glass. For the air passage, Perspex is chosen. This is because Perspex is unbreakable and hardly gets scratches. Perspex will be used for the Savonius rotor housing and the chimney.

6.3.6 Plastic Pipe Savonius Rotor

Plastic pipe is a widely used as thermoplastic polymer. It is widely used nowadays because plastic pipe is;

- Cheap
- Durable
- Light weight
- Easy to assemble

In this project, the Plastic Pipe is used to fabricate the Savonius rotor due to its light weight, high strength and low reactivity. All these are the main criteria needed for the Savonius rotor.

CHAPTER 7

MATHEMATICAL MODELING

7 MATHEMATICAL ANALYSIS

The preliminary design of the system is represented by the drawing in Figure 7.1 where the hot flue gas passes underneath the panel will be absorbed by the absorber. The whole system will be represented by mathematical modeling. Mathematical modeling is a set of mathematical representation to study the behavior of the system under different conditions.

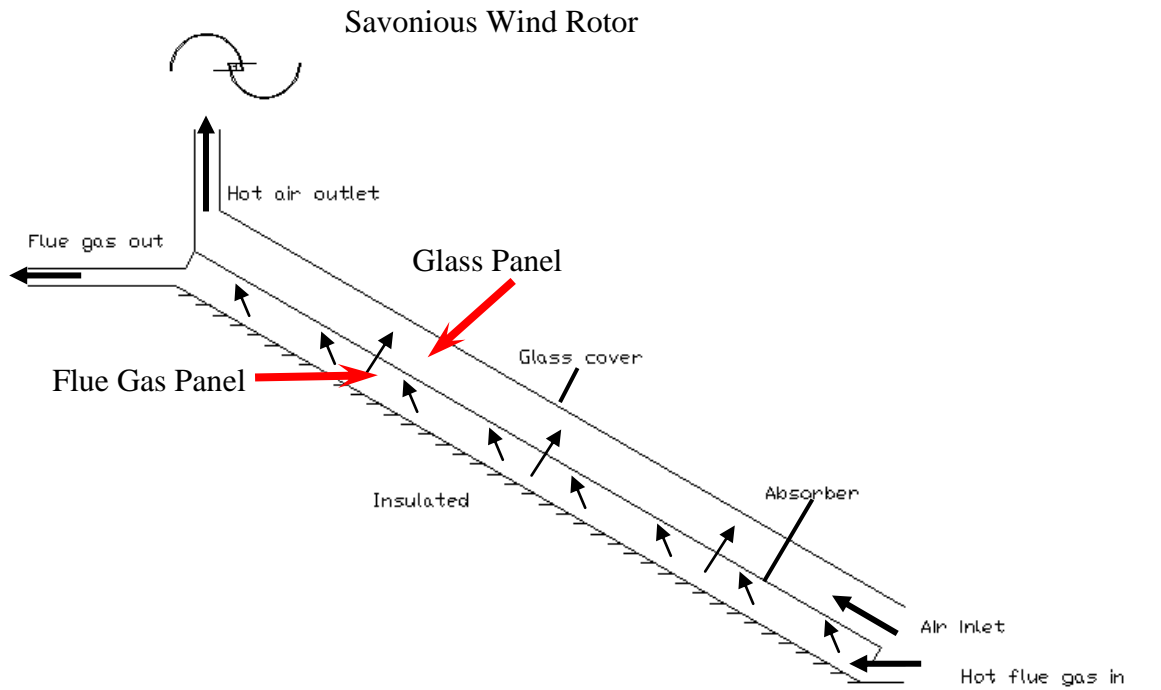


Figure 7.1: Side View of the Panel

Assumptions are needed in this mathematical analysis to simplify the overall process. There are several assumptions made before starting the analytical analysis for the panel:

1. No heat loss of flue gas from exhaust to the inlet of the panel
2. Constant heat flux throughout the process
3. Absorber plate with corrugated shape
4. For the noncircular cross sectional area, the convection coefficient is an average over the perimeter
5. Properties of air and flue gases are evaluated as a function of temperature
6. Products of the flue gas come from complete combustion process
7. Panel is well insulated at the bottom and side part
8. Heat losses only occur on the top part of the panel

7.1 Design Parameters of the Panel

The dimensions of the panel are proposed in Table 7.1.

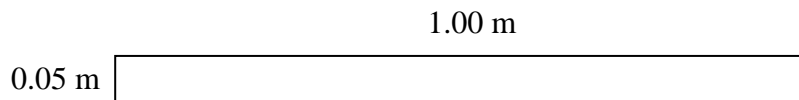
Table 7.1: Design Parameters of the Panel

Flue Gas Panel			
Length of panel	L1	2	m
Width of panel	w1	1	m
Inclination of panel	θ	45	$^{\circ}$
Distance between panel and absorber plate	d1	0.05	m

Absorber plate			
Length of absorber plate	L2	2	m
Width of absorber plate	w2	1	m
Area of absorber plate	A_p	2	m^2

Glass panel			
Length of glass	L3	2	m
Width of glass	w3	1	m
Distance between glass and absorber plate	d3	0.05	m

Cross sectional area of the panel,



Flow Cross Sectional Area,

$$A_c = a.b$$

$$A_c = 0.05 \text{ m} \times 1.00 \text{ m}$$

$$A_c = \underline{0.05 \text{ m}^2}$$

Cross Sectional Area of the Plate,

$$A_p = l.w$$

$$A_p = 1.00 \text{ m} \times 1.50 \text{ m}$$

$$A_p = \underline{1.50 \text{ m}^2}$$

Hydraulic Diameter of Air Passage,

$$D_{h,air} = 4A_c / P$$

$$D_{h,air} = 4 \times 0.05 \text{ m}^2 / (0.05 \text{ m} + 0.05 \text{ m} + 1.00 \text{ m} + 1.00 \text{ m})$$

$$D_{h,air} = \underline{0.0952 \text{ m}}$$

Area of the corrugated absorber plate



$$\text{Corrugated Plate Area} \sim \pi/2 \times \text{Flat Area}$$

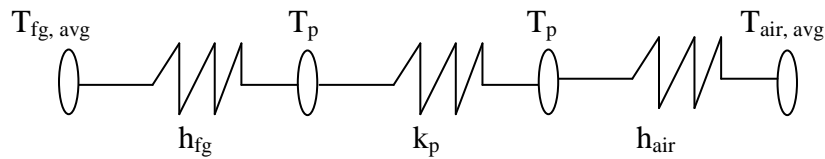
$$\text{Corrugated Plate Area} \sim \pi/2 \times 1.50 \text{ m}^2$$

$$\text{Corrugated Plate Area} = \underline{2.357 \text{ m}^2}$$

For corrugated plates, the area is multiply by $\pi/2$ due to its semi circular shape. From the results, we fixed the heat absorbed by the panel, and we can see a significant drop in flue gas temperature which is the main objective of the whole project. Therefore, corrugated plate is proposed for the design to improve on the heat absorbed efficiency.

7.2 Heat Transfer for the Panel

From Figure 7.1, the flue gas at will flow underneath a glass panel. This hot flue gas will transfer the heat to the absorber by heat convection. The heat transfer is modeled as below;



All properties of the flue gas and air are evaluated at its mean temperature. Accordingly, the mean temperature varies linearly with the length along the passage since we are assuming constant surface heat flux.

7.2.1 Heat Transfer in Flue Gas Passage

The calculation starts from the hot flue gas passage. An outlet temperature of flue gas is assumed to calculate the heat contained in the flue gas. All the flue gas properties are obtained from the mean temperature in the passageway.

$$T_{fg, in} = 850 \text{ K}$$

$$T_{fg, out} = T_{fg, out}'$$

$$Q_{fg} = m_{fg} \cdot c_{p, fg} \cdot (T_{fg, in} - T_{fg, out}')$$

After calculating the heat of the flue gas, we need to determine the Reynolds number and Nusselt Number to calculate for the heat transfer coefficient, h of the flue gas to the absorber. The equations used are shown below;

$$Re_D = \frac{\rho V D_H}{\mu}$$

For $Re_D > 2300$, the flow is turbulent. For fully developed turbulent flow, friction factor which is the function of surface condition for a wide range of Reynolds number must be obtained. The equation has been developed by Petukhov [8] and it is in the form of;

$$f = (0.790 \ln Re_D - 1.64)^{-2}$$

The convection correlation for the flow is given below. We use a correlation for a large Reynolds number range including the transition region provided by Gnielinski [8] to determine the Nusselt Number, Nu_D . The error of using this correlation is around 10%.

$$Nu_D = \frac{(f/8) (Re_D - 1000) Pr}{1 + 12.7(f/8)^{1/2} (Pr^{2/3} - 1)}$$

For laminar; $Nu_D = 4.86$

For turbulent; $Nu_D = \frac{(f/8) (Re_D - 1000) Pr}{1 + 12.7(f/8)^{1/2} (Pr^{2/3} - 1)}$

$$h = \frac{Nu_D \cdot k}{D_h}$$

7.2.2 Heat Transfer in Air Passage

The heat absorbed by the absorber will be transferred to the air by heat convection. The heat will increase the velocity of the moving particles and reduce its density at the same time. Thus, the warm air will move upward to achieve a desired outlet velocity of 4 to 5 m/s to generate the Savonius rotor.

Initially an outlet temperature of the air is assumed to calculate for the average temperature in the panel. This is important because all the properties of air are evaluated at the mean temperature in the panel.

$$\begin{aligned}T_{\text{air,in}} &= 300 \text{ K} \\T_{\text{air,out}} &= T_{\text{air,out}}' \\ \Delta T_{\text{air}}' &= T_{\text{air,out}}' - 300 \text{ K}\end{aligned}$$

Then it is important to determine the Grashof number, Reynolds number and Raleigh number to investigate if the air flow has a natural convection flow or by forced convection.

$$\begin{aligned}Re_{D,\text{air}} &= \frac{\rho_{\text{air}} \cdot V_{\text{mean}} \cdot D_{h,\text{air}}}{\mu_{\text{air}}} \\ Re_{L,\text{air}} &= \frac{\rho_{\text{air}} \cdot V_{\text{mean}} \cdot L}{\mu_{\text{air}}} \\ Gr_L &= \frac{g\beta (T_s - T_a)L^3}{\nu^2}\end{aligned}$$

For convection flow in a parallel plate channel,

$$\begin{aligned}Ra_D &= \frac{g\beta (T_s - T_a)d^3}{\alpha\nu} \\ Ra_L &= \frac{g\beta (T_s - T_a)L^3}{\alpha\nu}\end{aligned}$$

For an inclined channel, experiments have been performed by Azevedo and Sparrow [8]. For $0 \leq \theta \leq 45^\circ$, the Nusselt number of the flow can be obtained by using the correlated to within 10% of error by;

By natural convection; $Nu_D = 0.645 [Ra_D (d/L)]^{1/4}$

By forced convection; $Nu_{D} = 0.664 Re_D^{0.5} Pr^{1/3}$

Thus
$$h_{air} = \frac{k_{air} \cdot Nu_{D,air}}{D_{h,air}}$$

There is heat loss from the flue gas transferred to the air passage by convection and radiation. Only a certain amount of heat will be absorbed by the air. For the calculation of heat loss and heat absorbed by the air, an assumed surface temperature is set for the first iteration. Assuming an ambient temperature, T_a of 305 K;

$$Q_{loss} = \varepsilon \times 5.67 \times 10^{-8} \times A_s (T_s' - T_a)$$

$$Q_{air} = Q_{fg} - Q_{loss} = h \cdot A_s (T_s' - T_a)$$

From the calculation, the surface temperature will be calculated again by using the actual heat absorbed by the air

$$T_s = T_a + \frac{(Q_{fg} - Q_{loss})}{h_{air} \cdot A_s}$$

Then comparing both T_s and T_s' ;

If $|T_s' - T_s| > 0.5^\circ\text{C}$, continue iteration using T_s' as T_s value

If $|T_s' - T_s| < 0.5^\circ\text{C}$, stop iteration

From the heat absorbed by the air, we can evaluate the ΔT of air between the outlet and the inlet.

$$Q_{\text{air}} = m_{\text{a}} \cdot c_{\text{p,a}} \cdot \Delta T_{\text{air}}$$

$$\Delta T_{\text{air}} = Q_{\text{air}} / (m_{\text{a}} \cdot c_{\text{p,a}})$$

An inlet velocity of air is assumed to be 1 m/s which will be verified by using energy equation.

Then comparing both ΔT_{air} and $\Delta T_{\text{air}}'$;

If $|\Delta T_{\text{air}}' - \Delta T_{\text{air}}| > 0.5^{\circ}\text{C}$, continue iteration using $\Delta T_{\text{air}}'$ as ΔT_{air} value

If $|\Delta T_{\text{air}}' - \Delta T_{\text{air}}| < 0.5^{\circ}\text{C}$, stop iteration

The outlet temperature of the flue gas can be verified by using overall equation;

$$Q_{\text{f}} = U \cdot A_{\text{s}} \cdot \Delta T_{\text{mean}}$$

$$\Delta T_{\text{mean}} = \frac{\Delta T_{\text{fg}} - \Delta T_{\text{air}}}{\ln(\Delta T_{\text{fg}} / \Delta T_{\text{air}})}$$

$$U = [1/h_{\text{fg}} + 1/k + 1/h_{\text{air}}]^{-1}$$

$$Q_{\text{f}} = m_{\text{fg}} \cdot c_{\text{p}} \cdot (T_{\text{fg,in}} - T_{\text{fg,out}})$$

$$T_{\text{fg,out}} = T_{\text{fg,in}} - (Q_{\text{f}} / m_{\text{fg}} \cdot c_{\text{p}})$$

7.3 Energy Equation

From the energy equation, we can calculate exit velocity of the panel. The initial inlet velocity is assumed to be 1 m/s.

$$\frac{Q_{\text{air}}}{m} + h_i + \frac{V_i'^2}{2} + gz_i = h_o + \frac{V_o^2}{2} + gz_o$$

$$h_i = c_{p,\text{air}} T_{\text{in}}$$

$$h_o = c_{p,\text{air}} T_{\text{out}}$$

$$V_o^2 = \frac{Q_{\text{air}}}{m} + [h_i - h_o] + \frac{V_i'^2}{2}$$

So,

$$m = \rho_i A_i V_i' = \rho_o A_o V_o$$

$$P_o = \rho_o R T_o$$

Therefore

$$\frac{P_i V_i A_i}{T_i} = \frac{P_o V_o A_o}{T_o}$$

$$V_i = (T_i / T_o) (P_o / P_i) V_o (A_o / A_i)$$

Then comparing both V_i and V_i' ;

If $|V_i' - V_i| > 0.5^\circ\text{C}$, continue iteration using V_i' as V_i value

If $|V_i' - V_i| < 0.5^\circ\text{C}$, stop iteration

The V_o is the outlet velocity at the panel that is used to rotate the Savonius wind rotor.

The results for the iterations are shown in Table 7.2. The iteration is carried out based on 5 different values of the mass flow rate of flue gas.

Table 7.2: Data for different value of mass flow rate of flue gas

m_{fg} (kg/s)	$T_{fg,out}$ (K)	T_s (K)	$T_{air,out}$ (K)	ΔT_{air} (K)	Q_{air} (W)	V_{ext} (m/s)
0.10	845.27	361.32	302.52	2.52	228.21	4.01
0.25	842.91	393.78	305.37	5.37	503.74	5.11
0.50	841.42	450.21	311.07	11.07	930.3	6.09
0.75	839.45	492.8	320.35	20.35	1497.89	7.07
1.00	836.58	536.63	332.87	32.87	2189.21	7.92

After the first iteration by varying the mass flow rate of the flue gas at inlet, the iteration is being continued by using Spreadsheet in Microsoft Excel Software for various area of absorber plate. The results are shown in Table 7.3.

Table 7.3: Flue Gas Outlet Temperature for Various Absorber Areas for $m_{fg} = 0.25\text{kg/s}$

Area (m ²)	$T_{fg,out}$ (K)	$T_{air,out}$ (K)	ΔT_{air} (K)	Q_{air} (W)	V_{ext} (m/s)
2.357	843.05	304.62	4.62	433.45	4.13
4.713	838.06	306.91	6.91	647.88	5.19
7.070	833.72	308.69	8.69	815.41	5.87
9.426	829.79	310.19	10.19	955.50	6.72
11.783	826.15	311.49	11.49	1077.43	7.90

The characteristic parameter of the whole system is governed by mass flow rate and temperature difference. The product of mass flow rate and temperature difference will be the driving force for the system.

After calculating the parameters for the panel design, a graph is plotted to determine the characteristic parameter of the panel.

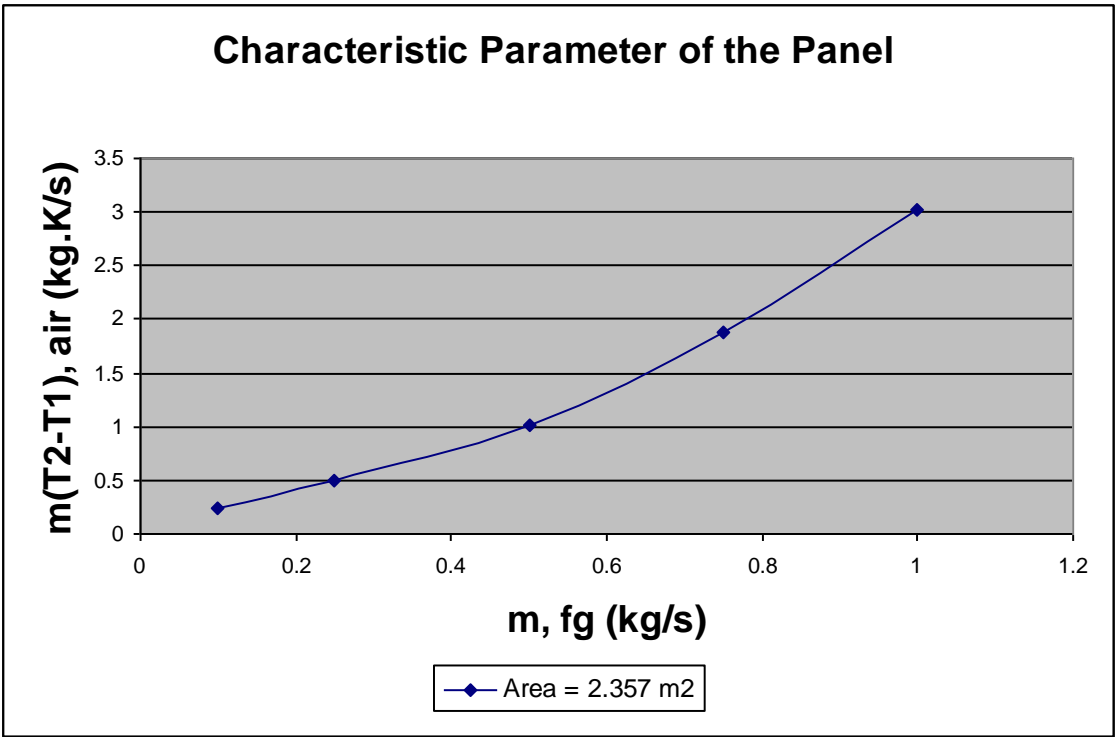


Figure 7.2: Characteristic Parameter of the Panel

As we can see from the graph, as the mass flow rate of the flue gas increases, the characteristic parameter increase as well. The temperature drop of the air becomes bigger. This is very important as the density of the air will decrease and thus increasing the buoyancy force.

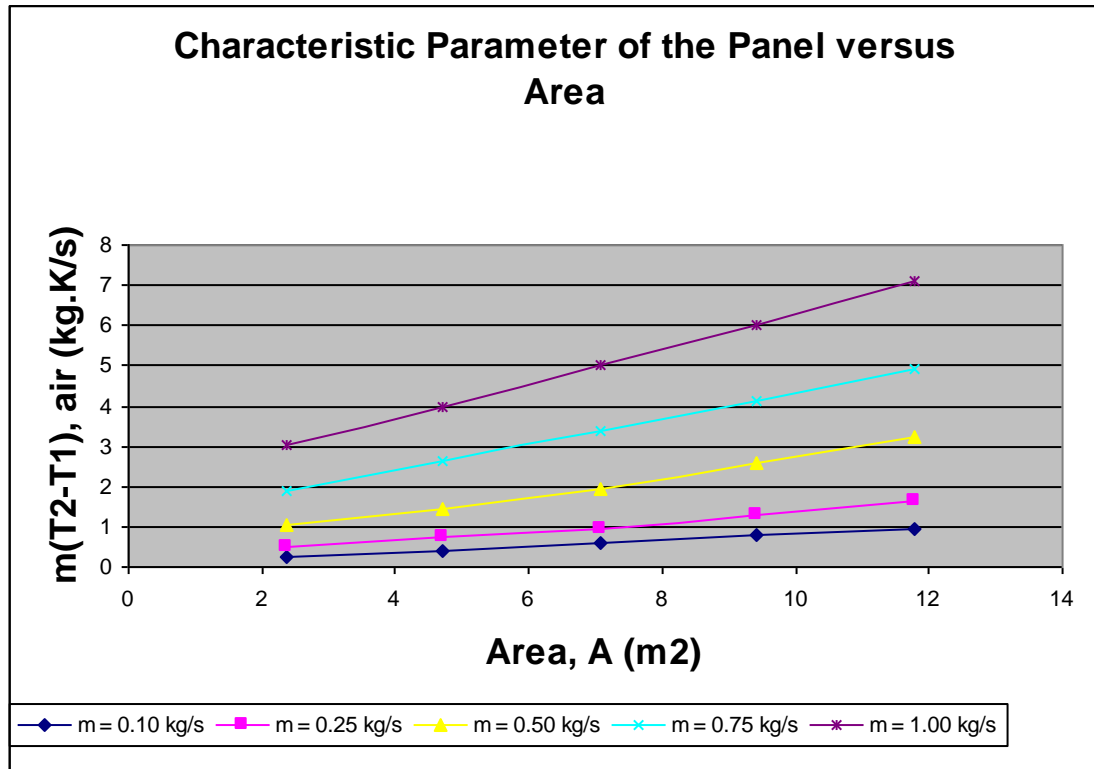


Figure 7.3: Characteristic Parameters of the Panel versus Area

For various sets of mass flow rate, we observe that the surface area for the absorber plays an important role here to control the characteristic parameter of the panel. As the surface area increases, the characteristic parameter increases as well.

However, from the analytical analysis, the changes in mass flow rate of the flue gas changes the characteristic material more significantly for this project.

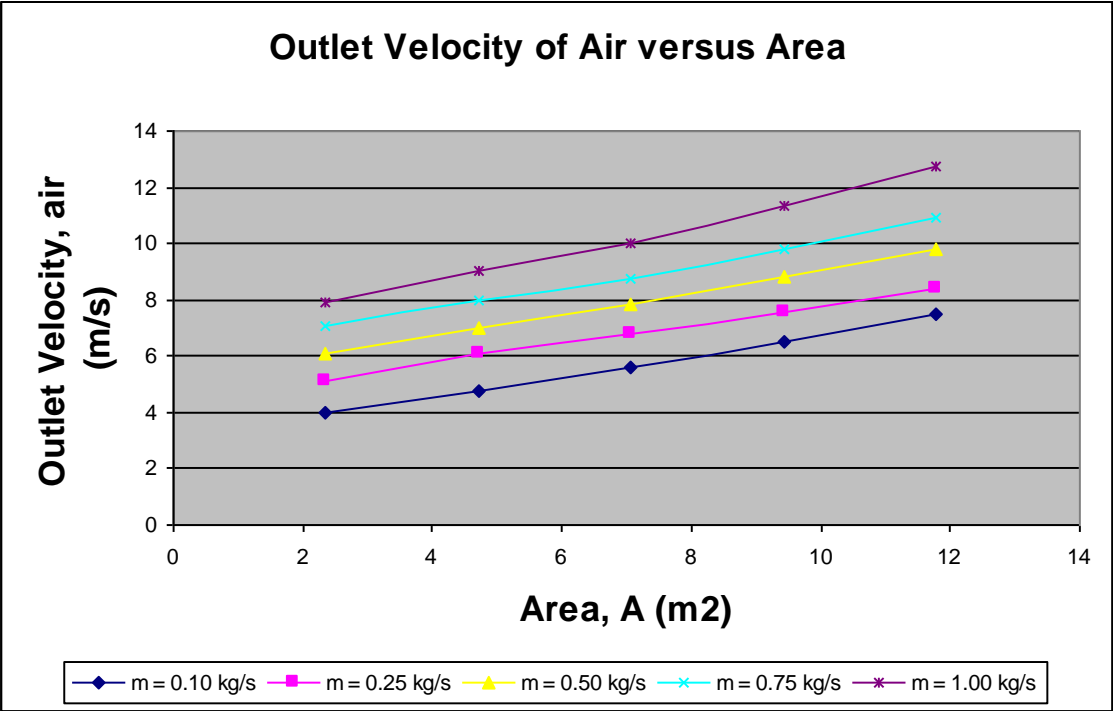


Figure 7.4: Outlet Velocity of air versus Area

If the area increases, more heat will be absorbed. This indicates that more heat will be transferred to the air passageway. Thus, air particles will be heated up and move upward at a higher velocity.

7.4 Power for Turbine

The exit velocity from the panel will be used to rotate the Savonius rotor.

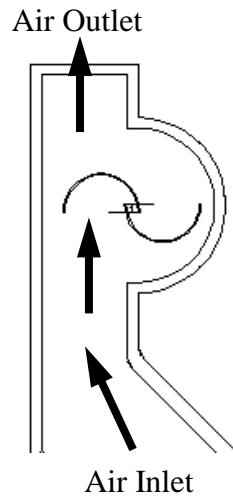


Figure 7.5: Air Flowing Through the Savonius Rotor

The kinetic energy generated from the air is given as;

$$P_{\text{air}} = \frac{1}{2} m_{\text{air}} \cdot V_{\text{air}}^2 \text{ (W/m)}$$

Depending on the configuration and type of Savonius rotor, we can evaluate the Turbine Power by using the Power Coefficient, $C_{p,\text{rotor}}$. For this project, the Savonius rotor follows the traditional configuration.

Analytically, the average power coefficient for this chosen design is 0.4. Therefore, the power output generated by the turbine is approximated as;

$$P_{\text{turbine}} = C_{p,\text{rotor}} \cdot P_{\text{air}} \text{ (W/m)}$$

The Power of the Turbine is evaluated based on 1 meter length. The calculated values for the turbine power and are shown in Table 7.4.

Table 7.4: Power Generated by the Rotor

m_{air} (kg/s)	V_o (m/s)	P_{input} (W/m)	P_{air} (W/m)	$C_{p,\text{rotor}}$	P_{turbine} (W/m)
0.10	3.75	727.19	0.6548	0.4	0.2619
0.25	5.13	2121.55	1.2253	0.4	0.4901
0.50	6.39	4595.42	1.9011	0.4	0.7605
0.75	8.03	7184.72	3.0022	0.4	1.2009
1.00	9.02	9822.68	3.7881	0.4	1.5153

The efficiency of the rotor depends mainly on its fabrication and installation. The rotor must achieve eccentricity and light weight materials must be used to reduce the rotation friction. From the values calculated, we observed that the efficiency of the system is very low which is around 0.02 % up to 0.03 %. Although the efficiency is very low, but this exploitation work is significant where we can utilize the heat waste for an application instead of letting it go to the atmosphere as a loss.

7.5 Force from the Chimney

There will be chimney installed on the top of the panel to create additional driving force to the Savonius rotor. The important parameters for the design of chimney are the height of the chimney, the design of the chimney and the exit area of the chimney.

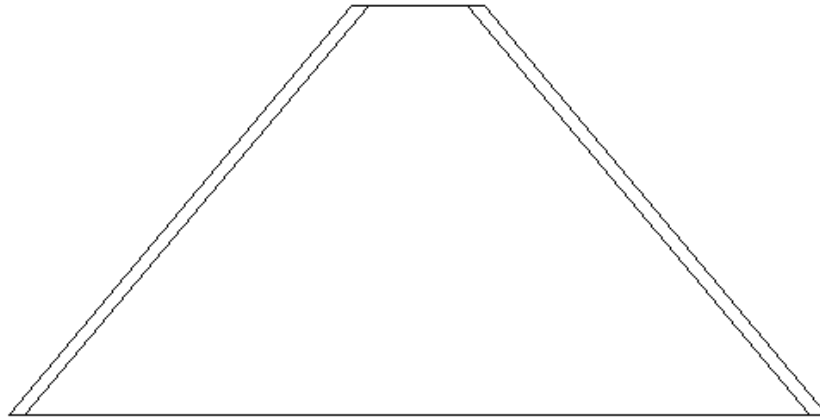


Figure 7.6: Proposed Chimney Design

Figure 7.6 shows the proposed chimney design for the system. The main intention to reduce the exit area of the chimney is to increase the exit velocity. Applying Bernoulli Equation, the pressure at the exit will be lower. Therefore we will have higher pressure drop to create higher driving force on the rotor. Besides that, the height of the chimney can be reduced as well.

Since $\Delta P = f(H, A_{out})$

$$\Delta P = \rho \cdot g \cdot \Delta H$$

where P is the pressure in the chimney, ρ is the density of the air, g is the gravitational acceleration and H is the height of the chimney.

The base length of the chimney will be 1 m and the top part will be 0.1 m.

Hence the area for the base and top part is calculated as below;

$$A_{\text{base}} = l \times w$$

$$A_{\text{base}} = 1 \text{ m} \times 0.03 \text{ m} = \underline{0.03 \text{ m}^2}$$

$$A_{\text{top}} = l \times w$$

$$A_{\text{top}} = 0.1 \text{ m} \times 0.03 \text{ m} = \underline{0.003 \text{ m}^2}$$

Bernoulli's equation can be used to determine the pressure drop in the chimney.

$$\frac{P_1}{\rho g} + \frac{V_1^2}{2g} + z_1 = \frac{P_2}{\rho g} + \frac{V_2^2}{2g} + z_2$$

$$z_1 - z_2 = \frac{P_2 - P_1}{\rho g} + \frac{V_2^2 - V_1^2}{2g} + h_{f,loss}$$

From the equation, it is clearly stated that the pressure drop in the chimney will increase as the height, H increases. As proposed, the chimney height will be 1.0 m for this design. From the properties, we can calculate the velocity at the base and top part of the chimney by using the mass flow rate.

$$m = \rho \cdot A \cdot V$$

For the base part, $m = \rho \cdot A \cdot V_{\text{base}}$

For the top part, $m = \rho \cdot A \cdot V_{\text{top}}$

$$V_{\text{avg}} = (V_{\text{base}} + V_{\text{top}}) / 2$$

After calculating the velocities, we need to determine the major and minor head loss in the chimney.

$$\text{Head loss, } h_f = f (L/D) \cdot (V_{\text{avg}}^2/2g)$$

The friction factor corresponds to the relative roughness and the Reynolds number. The value of friction factor can be determined from the Moody Chart using Colebrook's equation;

$$\frac{1}{\sqrt{f}} = -2.0 \log \left(\frac{\varepsilon/D}{3.7} + \frac{2.51}{\text{Re} \sqrt{f}} \right)$$

$$\varepsilon/D = 0 \text{ (smooth surface)}$$

By using equation solver or an iterative scheme, the friction factor can be determined from the Moody Chart.

The calculated values are shown in Table 7.5.

Table 7.5: Pressure Drop in the Chimney

m_{air} (kg/s)	Friction Factor (f)	Pressure Drop (Pa)
0.10	0.0115	682.21
0.25	0.0110	845.75
0.50	0.0108	1050.36
0.75	0.0102	1248.25
1.00	0.0096	1464.94

7.6 Experimental Results

The figure below shows the set up of the laboratory scale panel. Some other pictures are shown in Appendix IV.



Figure 7.7: Lab Scale Model Set Up

Area of the panel = 2.3565 m²

Mass flow rate of the flue gas = 0.18 kg/s

Table 7.6: Parameters for $m_{fg} = 0.18$ kg/s

Parameters	T = 20 minutes	T = 40 minutes	T = 60 minutes
$T_{fg,in}$ (K)	603	843	983
$T_{fg,out}$ (K)	599	838	973
$T_{air,in}$ (K)	293	293	293
$T_{air,out}$ (K)	297.8	300.5	307.8
$V_{air,in}$ (K)	0.9	0.9	0.9
$V_{air,out}$	1.7	3.5	4.1

Area of the panel = 2.3565 m²

Mass flow rate of the flue gas = 0.24 kg/s

Table 7.7: Parameters for mfg = 0.24 kg/s

Parameters	T = 20 minutes	T = 40 minutes	T = 60 minutes
T _{fg,in} (K)	611	848	995
T _{fg,out} (K)	604	840	983
T _{air,in} (K)	293	293	293
T _{air,out} (K)	299.2	303.5	310.6
V _{air,in} (K)	0.9	0.9	0.9
V _{air,out}	1.9	3.9	4.8

The data obtained is by experimental work for a flue gas mass flow rate of 0.18 kg/s and 0.25 kg/s with respect to time. As observe, the velocity of the air flowing at the panel exit increases with time.

$$\text{Percentage of error} = \frac{|5.11 \text{ m/s} - 4.8 \text{ m/s}|}{5.11 \text{ m/s}}$$

$$\text{Percentage of error} = \underline{\underline{6.06 \%}}$$

This percentage of error indicates that there are several errors occurred while conducting the experimental work.

7.7 Justification

Initially, this project analyzes the composition of the flue gases. We need to determine the properties of the flue gases to calculate the heat transfer analytically. From the analytical calculation, the mass flow rate of the flue gas and area of the panel are varied to observe the characteristic parameter of the panel.

The main objective of this project is to achieve an outlet air velocity of 4 to 5 m/s. This velocity of air will be able to rotate a Savonius rotor depending on the fabrication and the eccentricity. This parameter will be able to generate 0.5 W/m with an installation of generator. Thus, from the calculated value, this laboratory model will be scaled up to meet the desired power requirement.

The fabricated model has the proposed dimensions used for the analytical calculation. An early stage of experimental work is done to validate the calculated values. Based on the experimental data, the outlet velocity of air is around 3.5 to 4 m/s. The value obtained is lower than the calculated value. This indicates that there is some errors occurred while conducting the experiment. First of all, the ambient temperature while conducting the experiment is low as it is done in an air-conditioned space.

Another main problem is the fabrication of the Savonius rotor. It is proposed to use the CNC machine to cut a groove on the Perspex for eccentricity. However, due to the broke down of the machine, the semicircular plastic pipe is attached to the Perspex by using chloroform. Thus, it is difficult for the rotor to rotate due to the high friction of rotation. Thus, this analysis will be further developed for improvement.

CHAPTER 8

ECONOMIC EVALUATION & RECOMMENDATION

8 SOCIAL AND ECONOMIC JUSTIFICATION

Electricity can be generated from any type of heat source. Thus, the exploitation of the flue waste heat is an important task to convert them into another type of useful energy. The heat waste generated depending on the type of fuel source and power plant size.

There are some comparisons for different types of renewable energy as shown in Table 8.1.

Table 8.1: Comparisons between Several Type of Renewable and Recycled Energy [15]

Type	Energy Source Availability	Conversion Efficiency	Emissions Generated	Tax Credit
Renewable Energy				
Solar	25 %	25 % to 35 %	No	Yes
Wind	25 %	25 % to 35 %	No	Yes
Geothermal	100 %	5 % to 15 %	No	Yes
Hydro	100 %	25 % to 35 %	No	Yes
Biomass	100 %	25 % to 35 %	Yes	Yes
Recycled Energy				
Waste heat	100 %	25 % to 35 %	No	No

Table 8.1 shows that waste heat from the power plant can be a valuable source of thermal energy. Therefore, waste heat recovery has a potential to be classified as a priceless renewable energy in the future. It is not only saving the world's energy but also saving the environment at the same time.

8.1 Advantages

The main advantages for this project are:

1. Power generating with zero emission
2. Reduce CO₂ emission up to 20%
3. Help to save environment by reducing the heat escaped to the atmosphere
4. Help to reduce global warming issue
5. Increase the power plant efficiency by converting the thermal energy of flue gas into electricity
6. Economical for 1MW to 25MW Power Plants
7. Low capital cost project
8. Future renewable energy advantages

8.2 Future Recommendations

After finishing this project in this one year, there are a few recommendations proposed for future work to improve on the project.

8.2.1 Properties Distribution

This project needs a detail study of Pressure, Temperature and Velocity distribution for the panel experimentally and by CFD simulation. Computer simulation and experimental work can be used to validate the analytical part. From the computer simulation, we can easily identify the heat flow and velocity of air in the panel.

8.2.2 Fabrication of the Savonius rotor

We need to improve the fabrication of Savonius rotor by using CNC machine to achieve eccentricity. This is important to increase the efficiency of the rotor as well as the power output.

8.2.3 Traditional rotor

We can try to use different types of rotor to evaluate the effectiveness of this project. The overall performance of this project may increase by using traditional rotor instead of Savonius rotor.

8.2.4 Installing fins on the absorber plate

There are several ways to improve on the heat transfer associated with internal flow. This can be achieved by increasing the convection surface area or increasing the heat transfer coefficient, h . Therefore, for this project, I would recommend a future work to install fins on the absorber plate to increase the surface area.

8.2.5 Higher pressure gradient

A higher pressure gradient can be achieved by installing the panel exit back to the chimney stack. Therefore, we can eliminate the installation of high chimney on the panel. This will have to be examined further to increase its effectiveness.

CHAPTER 9

CONCLUSION

9 CONCLUSION

Flue gas emission from thermal power plant contributes significantly to the increasing of global temperature. Thus, energy recovery by conversion of thermal energy of the flue gas to electricity is an essential study nowadays.

The mathematical modeling for the whole system has been done with some suggested improvements to make the system more efficient. The 2 Dimensional and 3 Dimensional designs drawing for the system are drawn. After the analytical part and design drawing, the prototype is fabricated for experimental purpose. An outlet velocity at 4m/s can be achieved by experimental examination.

In conclusion, I managed to achieve all the objectives for this whole project and further developments have been proposed for further improvement.

REFERENCES

- [1] Babcock & Wilcox Co. (2005). *Steam: Its Generation and Use*, 41st edition. ISBN 0-9634570-0-4
- [2] June 13, 2006, <<http://www.eas.asu.edu/~holbert/eee463/FOSSIL.HTML#top>>
- [3] <http://library.thinkquest.org/3646/earth/resources/fosfuels.html>
- [4] <http://www.naftc.wvu.edu/technical/indepth/LPG/LPG.html>
- [5] EIA 2007 Annual Energy Outlook
- [6] Summer 2005 titled “Energy Matters” by Arvind Thekdi – E3M, Inc. and Energy Matters Editorial Advisory Board member and Richard Bennett – Janus Technology Group
- [7] www.modares.ac.ir/elearning/Sadramel/IHRS/files/Chap1-intro.pps
- [8] Incropera F.P., DeWitt D.P., Bergman T.L. and Lavine A.S., 2007. Introduction to Heat Transfer, 5th Edition, John Wiley & Sons, New York
- [9] Hussain H. Al-Kayiem (A.P. Dr.), Afreen E. Sa’ad Al-Deen, *Performance Analysis of Savonius Wind Rotor for Ducted Flow Operation*, Accepted for Publication, 2007, Malaysia
- [10] Dr. Alan Williams, *The Solar Nozzle – a possible approach for Efficient, Large Scale, Solar Electricity*, November 2007
- [11] M. M. Padki and S. A. Sherif, International Journal of Energy Research, 1999, 23, page 345-349
- [12] P K NAG, 2002. Power Plant Engineering, 2nd Edition, McGraw-Hill
- [13] W. Shepherd and D. W. Shepherd, 2003. Energy Studies, 2nd edition, Imperial College Press.
- [14] Yunus A. Cengel and Michael A. Boles, 2006. Thermodynamics, An Engineering Approach, 5th Edition, McGraw-Hill
- [15] James.S. Wallace, " Assessment of" First Generation Propane Conservation Equipment," S.A.E Paper N. 892144
- [16] Colin R. Ferguson, Internal Combustion Engines, John Willey & Sons, Inc. 1986
- [17] http://www.engineeringtoolbox.com/fuels-exhaust-temperatures-d_168.html

APPENDICES

Nomenclature

Q_{fg}	Heat released by the flue gas
Q_{abs}	Heat absorbed by the plate
Q_{air}	Heat absorbed by the air particles
m_{fg}	Mass flow rate of flue gas
ρ_{fg}	Density of flue gas
$c_{p,fg}$	Specific heat of flue gas
μ_{fg}	Viscosity of flue gas
k_{fg}	Thermal conductivity of flue gas
$Pr_{,fg}$	Prandtl Number of flue gas
V_{fg}	Velocity of flue gas
$D_{h,fg}$	Hydraulic diameter of the flue gas passage
$T_{fg,in}$	Temperature of flue gas at inlet
$T_{fg,out}$	Temperature of flue gas at outlet
$T_{fg,avg}$	Average temperature of flue gas
$Re_{,fg}$	Reynolds number of flue gas
$Nu_{,fg}$	Nusselt Number of flue gas
h_{fg}	Convection coefficient of flue gas
A_c	Cross sectional area
A_s	Surface area
A_p	Area of the plate absorber
T_{abs}	Temperature of the absorber
m_{air}	Mass flow rate of air
ρ_{air}	Density of air
$c_{p,air}$	Specific heat of air
μ_{air}	Viscosity of air
k_{air}	Thermal conductivity of air

$Pr_{,air}$	Prandtl Number of air
β	Thermal expansion of air
V_{air}	Velocity of air
$D_{h,air}$	Hydraulic diameter of the air passage
$T_{air,in}$	Temperature of air at inlet
$T_{air,out}$	Temperature of air at outlet
$T_{air,avg}$	Average temperature of air
$Re_{,air}$	Reynolds number of flue gas
$Nu_{,air}$	Nusselt Number of flue gas
h_{air}	Convection coefficient of flue gas
Gr_L	Grashof Number throughout the air flow
Re_L	Reynolds Number throughout the air flow
P_{air}	Power of flowing air
$P_{turbine}$	Power of the turbine
$C_{p,rotor}$	Power coefficient of the rotor

Appendix I

Experienced Exhausts Temperature [3]

Appliance Type	Exhaust Temperature	
	(°F)	(°C)
Chemical Oxidation	1350 - 1475	730 - 800
Annealing Furnace	1,100 - 1,200	590 - 650
Fluidized-bed Combustor	1,600 - 1,800	870 - 980
Natural-gas fired heating appliance with draft hood	360	182
Liquefied-petroleum gas-fired heating appliance with draft hood	360	182
Gas-fired heating appliance, no draft hood	460	238
Glass melting furnace	1,200 - 1,600	650 - 870
Oil-fired heating appliance, residential	560	293
Oil-fired heating appliance, forced draft over 400,000 Btu/h	360	182
Conventional incinerator	1,400	760
Controlled air incinerator	1,800 - 2,400	982 - 1,316
Pathological incinerator	1,800 - 2,800	982 - 1,538
Gas turbine exhaust	700 - 1,100	370 - 590
Diesel exhaust	1,000 - 1,200	540 - 650
Ceramic kilns	1,800 - 2,400	982 - 1,316

Appendix II

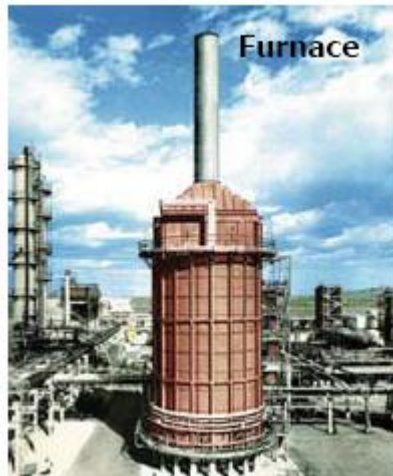
Types of heat waste source;



Refinery

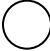
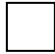
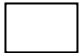
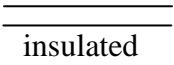



Furnace



APPENDIX III

Nusselt Number and Friction Factors for Fully Developed Laminar Flow in Tubes for Non Circular Cross Section [8]

Cross Section	b/a	$Nu_D = h \cdot D_h / k$		$f Re_{Dh}$
		Uniform q''	Uniform T_s	
	-	4.36	3.66	64
a  b	1.0	3.61	2.98	57
b a 	1.43	3.73	3.08	59
	2.0	4.12	3.39	62
	3.0	4.79	3.96	69
	4.0	5.33	4.44	73
	8.0	6.49	5.60	82
 insulated	∞	5.39	4.86	96
	-	3.11	2.49	53

Used with the permission from W.M. Kays and M.E. Crawford, *Convection Heat and Mass Transfer*, 3rd Edition, McGraw-Hill, New York, 1993.

APPENDIX IV

Actual panel model;



